INTEGRAL BRIDGES

SOIL-STRUCTURE INTERACTION

Jaromir Krizek

PREFACE

Handbook “Integral Bridges Soil-Structure Interaction” offers a practical tool for design of integral bridges. Integral bridges are structures without bearings and mechanical expansion joints, whereas the connection between the superstructure and the substructure is usually framed. Therefore, these bridges are considered as frame structures. Because of continuity between the superstructure and the substructure, there is a significant interaction with surrounding soil and backfill behind abutments, especially during thermal expansion, as the substructure is pushed into the soil of the backfill. The soil is represented as an elastic-plastic material which properties affect internal forces in the integral bridge structure. Therefore, it is necessary to consider correctly the influence of the soil in the integral bridge design. This is one of the main problems in the calculation of integral bridges in practice. A way, how to deal with the problem, is described in this handbook.

The handbook describes the method simulating the surrounding soil by a system of soil springs located to substructure elements. Practical usage of the method is demonstrated on several solved examples. You can find here detailed guideline, how to calculate the stiffness of these horizontal and vertical soil springs, which are located to abutments and spread foundations of integral bridges. The stiffness of the soil springs depend on dimensions of the superstructure and the substructure, on parameters of the surrounding soil and on the loading of the bridge. Consequently, you can use calculated values in a structural model of the integral bridge as values of stiffness of vertical and horizontal soil springs located to the elements of the substructure.

I believe that this handbook will become a useful aid in practical design of integral bridges and that it will contribute to their more frequent utilization.

Author

CONTENTS

LIST OF SYMBOLS AND ABBREVIATIONS

c	[kPa]	Soil cohesion
f	[kN/m^2]	Stress on the contact area between the solid pushed into the soil and the soil
f_{cd}	[MPa]	Design value of concrete compressive strength
f_{S0}	[kN/m]	Horizontal load of the abutments due earth pressures at rest
f_{UDL}	[kN/m]	Uniformly distributed load of the bridge due to traffic
f_x	[kN/m^2]	Horizontal stress in the footing bottom
$f_{x, lim}$	[kN/m^2]	Limit value of horizontal stress in the footing bottom
f_{yd}	[MPa]	Design yield stress of steel
f_z	[kN/m^2]	Vertical stress in the footing bottom
$f_{z, lim}$	[kN/m^2]	Limit value of vertical stress in the footing bottom
h_i	[m]	Thickness of the ith layer
k	[MN/m^3]	Modulus of subgrade reaction
k_h	[MN/m^3]	Horizontal modulus of subgrade reaction for abutments
k_x	[MN/m^3]	Horizontal modulus of subgrade reaction for spread footings
k_{xi}	[MN/m^3]	Horizontal modulus of subgrade reaction of ith layer below spread footing
k_{xs}	[MN/m^3]	Total horizontal modulus of subgrade reaction for layered subsoil below spread footing
k_z	[MN/m^3]	Vertical modulus of subgrade reaction for spread footing
k_{zi}	[MN/m^3]	Vertical modulus of subgrade reaction of ith layer below spread footing
k_{zs}	[MN/m^3]	Total vertical modulus of subgrade reaction for layered subsoil below spread footing
n	[-]	Modular ratio
u	[m]	Impression of the solid into the soil
u_r	[-]	Relative displacement
u_{rBx}	[-]	Relative horizontal displacement at the bottom of ith layer
u_{rBz}	[-]	Relative vertical displacement at the bottom of ith layer
u_{rTx}	[-]	Relative horizontal displacement at the top of ith layer
u_{rTz}	[-]	Relative vertical displacement at the top of ith layer
u_B	[m]	Horizontal displacement at the bottom of abutment
u_T	[m]	Horizontal displacement at the top of abutment
z	[m]	Depth below ground surface
z_2	[m]	Depth of points 2R, 2T and 2M below ground surface
z_B, z_T	[m]	Depth of points B and T below ground surface
z_r,	[-]	Relative depth below ground surface
z_{rB}, z_{rT}	[m]	Relative depth of points B and T below ground surface

A, B, C, D	[-]	Factors for calculation of horizontal reaction moduli on the abutments
A_{eff}	[m^2]	Cross-sectional area of the effective equivalent steel section
B_f	[m]	Width of spread footing
E_a	[MPa]	Modulus of elasticity of structural steel
E_c'	[MPa]	Effective modulus of elasticity for concrete
E_{cm}	[MPa]	Secant modulus of elasticity of concrete
E_{ref}	[MPa]	Reference stiffness modulus of soil
F_{TS}	[kN]	Load force due to tandem system
G	[-]	Load case due to self-weight
G_a	[-]	Load case due to self-weight of steel girder
G_c	[-]	Load case due to self-weight of the reinforced concrete slab
G_s	[MPa]	Shear stiffness modulus of soil
G_{fin}	[-]	Load case due to pavement and bridge equipment
G_k	[-]	Characteristic value of a permanent action
G_{ref}	[MPa]	Reference shear stiffness modulus of soil
GWL	[m]	Groundwater level
H_a	[m]	Height of abutment
H_s	[m]	Depth of compressible subsoil
I_D	[-]	Index of relative density of soil
$I_{eff,y}$	[m^4]	Second moment of area of effective equivalent steel section around major axis
K, L, M, N	[-]	Factors for calculation of vertical reaction modulus on the spread footing
K_h	[MN/m^2]	Horizontal stiffness of distributed elastic support located on abutment beam
K_x	[MN/m^2]	Horizontal stiffness of distributed elastic support located on footing beam
K_z	[MN/m^2]	Vertical stiffness of distributed elastic support located on footing beam
L	[m]	Span of superstructure
L_{tot}	[m]	Total length of bridge
L_f	[m]	Length of spread footing
P, Q, R, S, T, U	[-]	Factors for calculation of horizontal reaction modulus on the spread footing
Q_{k1}, Q_{k2}	[-]	Characteristic value of leading and accompanying variable action
S_0	[-]	Load case due to earth pressure at rest
S_r	[-]	Degree of saturation
T_0	[ºC]	Initial temperature of the bridge at time of installation
T_{max}	[ºC]	Maximum shade air temperature
$T_{e,\,max}$	[ºC]	Maximum uniform temperature component of the bridge
TEM	[-]	Load case due to thermal action
TS	[-]	Load case due to tandem system traffic load inducing maximal effect in the middle of the bridge span

TS_1,…, TS_{30}	[-]	Load cases due to tandem system traffic load inducing maximal effect in particular section of bridge superstructure
TS_{env}	[-]	Envelope of load cases TS_1 to TS_{30}
UDL	[-]	Load case due to uniformly distributed traffic load
W_x	[-]	Groundwater factor for calculation of horizontal reaction modulus on the spread footing
W_z	[-]	Groundwater factor for calculation of vertical reaction moduli on the spread footing
α_{q1}, α_{q2}	[-]	Adjustment factors for distributed traffic load on the bridge – UDL
α_{Q1}, α_{Q2}, α_{Q3}	[-]	Adjustment factors for concentrated traffic load on the bridge–Tandem System
α_t	[K^{-1}]	Factor of linear thermal expansion of steel and concrete
γ	[kN/m^3]	Soil unit weight
ΔL	[mm]	Thermal extension of the bridge
$\Delta T_{N, exp}$	[ºC]	Uniform temperature component for the bridge
ν	[-]	Poisson's ratio
φ	[º]	Friction angle of soil
σ_{max}	[MPa]	Maximal stress reached in the steel girder, in reinforcement and in concrete
ψ_1, ψ_2	[-]	Combination factors

1 INTRODUCTION

1.1 Concept of Integral Bridge

For centuries, bridges were constructed without any mechanical expansion joints and bearings. This changed at the turn of 19th and 20th century, when more or less simplified analysis models started to be used in the design of bridge structures and when stone, as a traditional construction material, was more and more replaced by steel and concrete. Expansion joints and bearings, which separate a superstructure from a substructure and which allow their relative displacement, became common parts of bridges. However, a lifespan of expansion joints and bearings is significantly lower than a lifespan of the rest of the bridge structure. The joints and the bearings bring often problems concerning their maintenance or possible replacement. In many countries, efforts to reduce operating costs lead to such structural design that eliminates using of expansion joins and bearings. The bridges without bearing and joints are termed **'integral'** [6]. The elimination of bearings and mechanical expansion joints is the main advantage of integral bridges considerable reducing their construction and operating costs. Because the connection of a superstructure to a substructure is usually framed, integral bridges are also called frame bridges [11]. Integral bridges became very popular in many countries. They are often used in Great Britain [12], Germany [7], [8], [18], [19], [20], [21], Sweden [9], [17], USA and other countries. Integral bridges are very good alternative to the traditional girder bridges with one or more short or medium spans.

1.2 Structural Arrangement

As already mentioned, integral bridges are specific when compared with traditional girder bridges, because they do not contain expansion joints and bearings. The elimination of these structural elements separating the superstructure from the substructure leads to many differences between integral bridges and traditional girder bridges. You can compare typical structural arrangements of traditional and integral bridge in Figure 1.1. The most important differences in structural arrangements of integral and traditional bridges are following:

1) Connection of the superstructure and the abutments,
2) Road transition between the bridge and adjacent embankment.

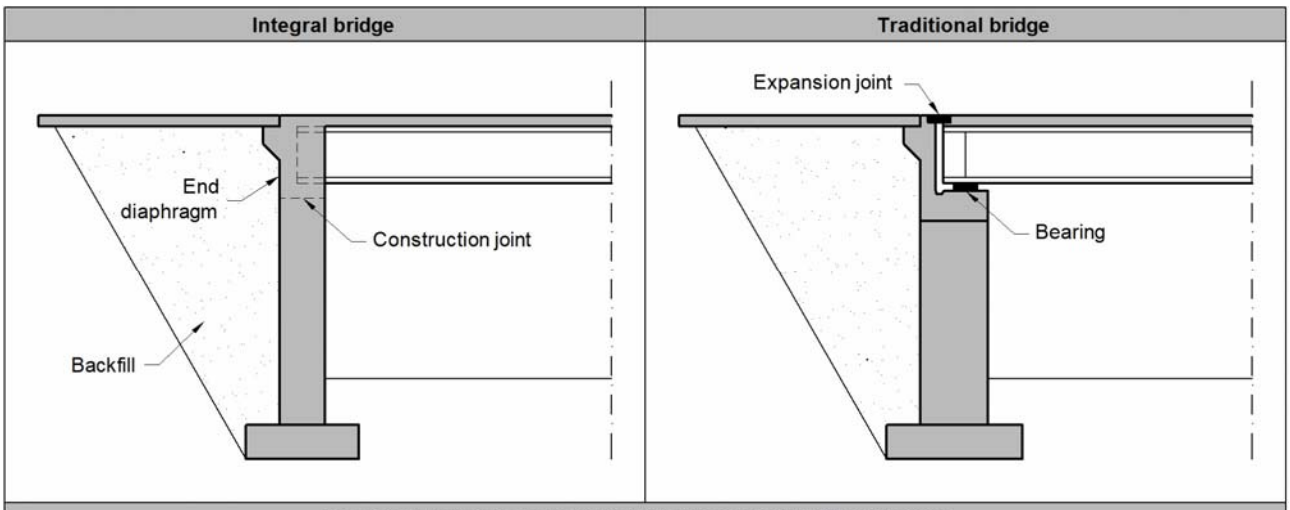

Fig. 1.1 Structural arrangement of integral and traditional bridge

In case of the traditional girder bridges, the superstructure is connected to the abutments by bearings. As for integral bridges, main girders are ended by diaphragm, which is fixed to an abutment. It forms a rigid frame joint. With regard to the road transition between the bridge and the adjacent embankment, in case of traditional bridges is necessary to use an expansion joint to span a gap between the superstructure and the abutment. As for integral bridges, the expansion joint as well as the gap is eliminated.

1.3 Statical Action

Differences in structural arrangements of integral bridges and traditional girder bridges lead to differences of their statical action. The most important differences are following:

1) Rigid frame joint between a superstructure and a substructure,
2) Interaction between the superstructure, the substructure and the surrounding soil,
3) Restraint of free expansion of the superstructure.

As for traditional bridges, the superstructure is supported by bearings, which allow free rotation of bridge ends; thereby the bearings represent hinged support independent on the geometry of the abutment. Expansion joints and bearings are usually arranged to allow free expansion in the longitudinal and sometimes in the transversal direction of the bridge due to temperature changes. It is reached by the usage of appropriate combination of fixed and sliding bearings.

Since the superstructure of integral bridge is fixed to the substructure, all displacements and rotations of the superstructure are transmitted to the substructure, see Figure 1.2.

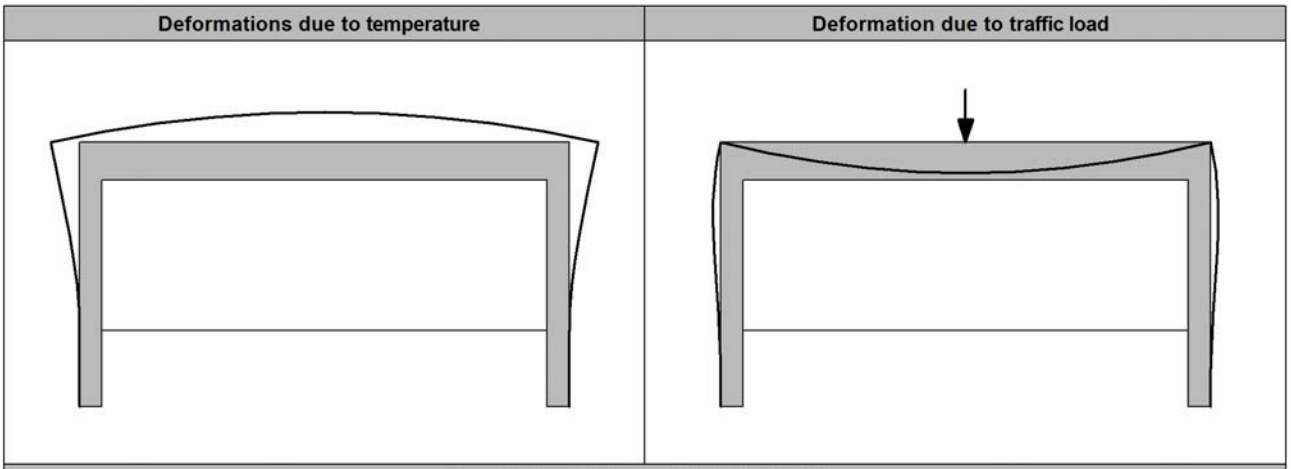

Fig. 1.2 Deformations of integral bridge

During the thermal expansion, the abutments are pushed into the soil of backfill, which brings about passive earth pressures acting on the abutments. The movements of the superstructure are restrained by the stiffness of the abutments and by the earth pressure acting on the abutments. This causes an interaction of the superstructure, the substructure and the surrounding soil.

1.4 Design

With regard to the structural arrangement and statical action of integral bridges, we can summarize the basic design differences of integral and traditional bridges as follows:

1) Inclusion of the superstructure, the substructure and the surrounding soil into a single structural model,
2) Significant influence of temperature changes on the stress state of the structure.

In case of traditional bridges, the connection of the superstructure and the abutments is usually hinged and the expansion joints and bearings allow relative movements between the superstructure and the substructure. Hence, the superstructure and the substructure can be analyzed separately, see Figure 1.3d.

In case of integral bridges, where the superstructure significantly interacts with the substructure, it is necessary to include the substructure into the structural model. The stiffness of the abutments influences a distribution of internal forces in the superstructure and in the abutments themselves. Thus, it is necessary to create a structural model including both the superstructure and the substructure, see Figure 1.3b.

Similarly as for the substructure, it is also necessary to include an influence of the backfill behind the abutments into the structural model of the integral bridge. As a result of abutment displacements due to thermal expansion, the soil behind abutments is compressed and influences stresses in the whole bridge structure. The influence of the backfill is considered by soil springs, which are located on the abutments. These soil springs are oriented horizontally, i.e. transverse to the back of the abutment.

The structural model of an integral bridge is a statically indeterminate frame, where internal forces are influenced by support settlements. In case of foundation on spread footing, it is appropriate to represent its flexibility by elastic springs located in the vertical and horizontal direction on the spread footing.

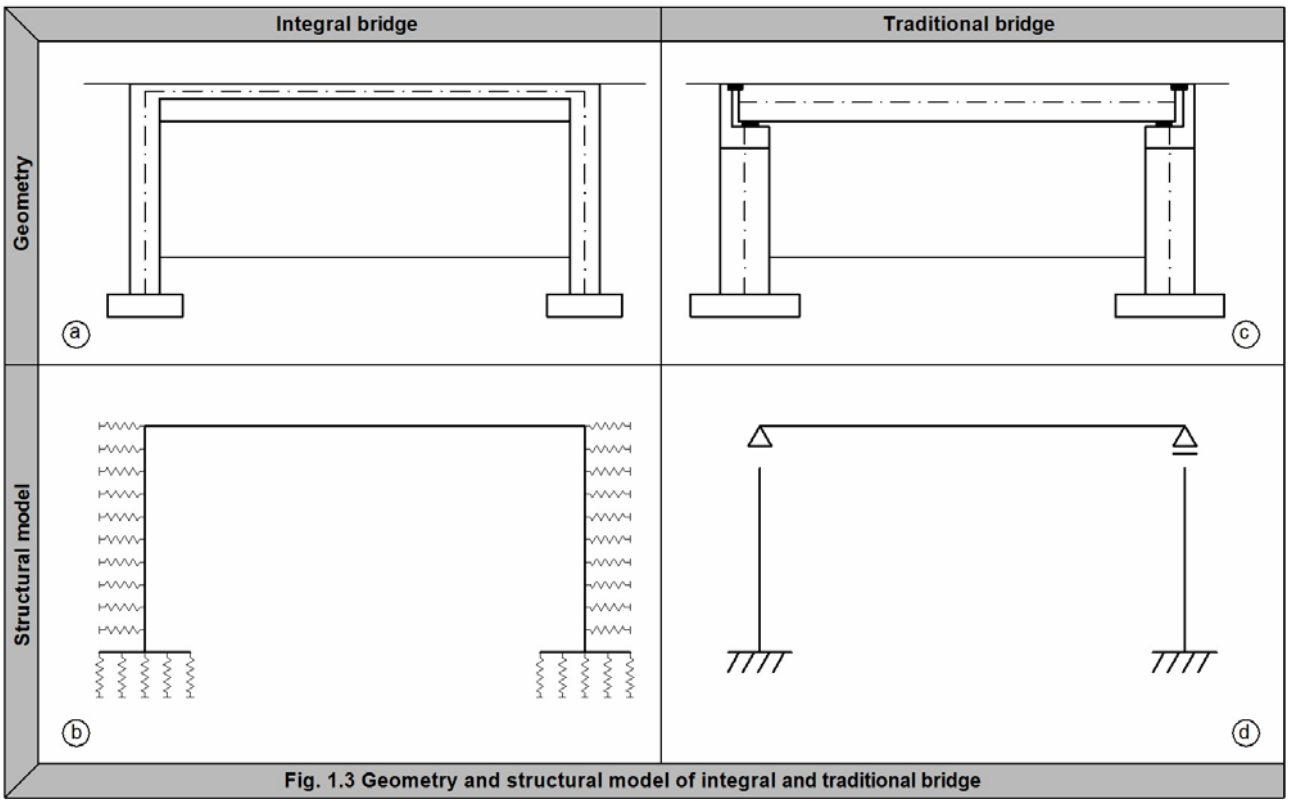

Fig. 1.3 Geometry and structural model of integral and traditional bridge

1.5 Usage and Advantages of Integral Bridges

Integral bridges become widely used in practice. Because of lower construction and maintenance costs and other advantages, they established themselves in economic competition in many countries. Integral bridges are currently often used in Germany, Sweden, Great Britain, USA and in other countries. According to the British standard [1], it is recommended to prefer integral bridges in such cases, where the total length of the superstructure is less than 60 m and the skews do not exceed 30°. The reason for the length limit of the superstructure is the absence of bearings and expansion joints. In case of longer spans, this structural arrangement could cause problems in the transition zone. It must be indeed pointed out, that bridges with the total length lower than 60 m occur most often in practice. However, integral bridges with the higher length than 60 m exist. In these cases, it is appropriate to use integral bridges with added expansion joints.

Integral bridges have many forms and wide range of utilization. They are applied as road bridges [21], railway bridges [8], but also as footbridges. In term of the number of spans, there are structures with one or more spans [18]. The superstructure can be carried out from reinforced concrete [11], from prestressed prefabricated concrete [13], [16], eventually composite with the reinforced concrete deck and steel main girders, either full-web [10] or truss [11]. However, the guiding principles described in the introduction as well as the method to calculate stiffness of soil springs (see below) is valid for all types of integral bridges.

The main advantages of integral bridges can be summarized as follows:

1) **Elimination of expansion joints and bearings:** The elimination of expansion joints and bearings lead to lower construction costs of the bridge. Since the expansion joints and bearings generally have lower lifespan than the superstructure, they require regular maintenance and need to be replaced several times during the bridge existence. In case of integral bridges, this problem is eliminated. Thereby it reduces operating costs and closures of the bridge due to maintenances are less often [17], [22].

2) **Simplified substructure:** The superstructure is monolithically connected to the abutments. This eliminates bearing pads, end screen walls and cross expansion gaps, because all is integrated into the end diaphragm. Moreover, the abutments are strutted by the superstructure and supported by the surrounding soil. This leads to higher stability of the substructure, to the possibility of design of slender abutments, to reduction of spread footings and, in case of pile foundation, to design of one row of piles only for each abutment. These simplifications of the substructure strongly reduce material consumption, earthworks volume and, consequently, the construction costs.

3) **Faster and simplified construction process:** In case of integral bridges, the works concerning keeping precise geometry of bearings and placement of mechanical expansion joints are eliminated. Together with the simplification of the substructure, it leads to faster and simpler construction of an integral bridge.

4) **Slender superstructure:** Because of the frame behavior of the structure, bending moments are redistributed from the sagging moments to hogging moments. It allows the design of a slenderer superstructure with reduced bridge superstructure depth in comparison with simply supported bridges.

5) **Shorter and lower highway ramps:** In case of bridges at interchanges in flat terrain, the above-mentioned reduction of the superstructure depth leads to shorter and lower highway ramps and embankments. It leads to further reduction of earth works [11].

6) **Drive comfort improvement:** Because of the elimination of expansion joints, a smooth road transition between adjacent embankment and the bridge is achieved. To avoid failures in a road transition, proper construction of the transition zone should be chosen.

7) **Remove of problematic details:** In case of traditional bridges, reactions from the superstructure to the substructure are transmitted by bearings. This leads to a strong concentration of stresses in bearing pads and bridge seats. In case of integral bridges, this problem is resolved because massive frame end-diaphragm is provided. Another advantage is the elimination of a possible leakage to the substructure through expansion joints [15].

8) **Robust structure:** The frame connection of the superstructure and the substructure increases the static indeterminacy and the structure robustness. Because of their higher ductility, integral bridges are more resistant to seismicity and other accidental actions, e.g. impacts of vehicles to the abutments, displacements of abutments due to floods, or terrorist attacks.

2 CALCULATION METHOD OF MODULI OF SUBGRADE REACTION

One of the problems of the practical design of integral bridges is the adequate consideration of the surrounding soil, which supports the substructure. If the subsoil is represented as a system of elastic soil springs located on the elements, which are in contact with the soil (see Figure 1.3b), a question arises how to determine the stiffness of these soil springs properly. Stiffness of soil springs can be calculated using following method.

In the method, the stiffness of soil springs is expressed by moduli of subgrade reaction. Physically, modulus of subgrade reaction represents stiffness of a surface spring supporting surfaces or solids. The definition of the modulus of subgrade reaction k is than following:

$$k = \frac{f}{u} \tag{2.1}$$

where: f is the stress on the contact area between the solid pushed into the soil and the soil,
u is the impression of the solid into the soil.

Figure 2.1 shows the moduli of subgrade reaction, which can be determined by means of this method.

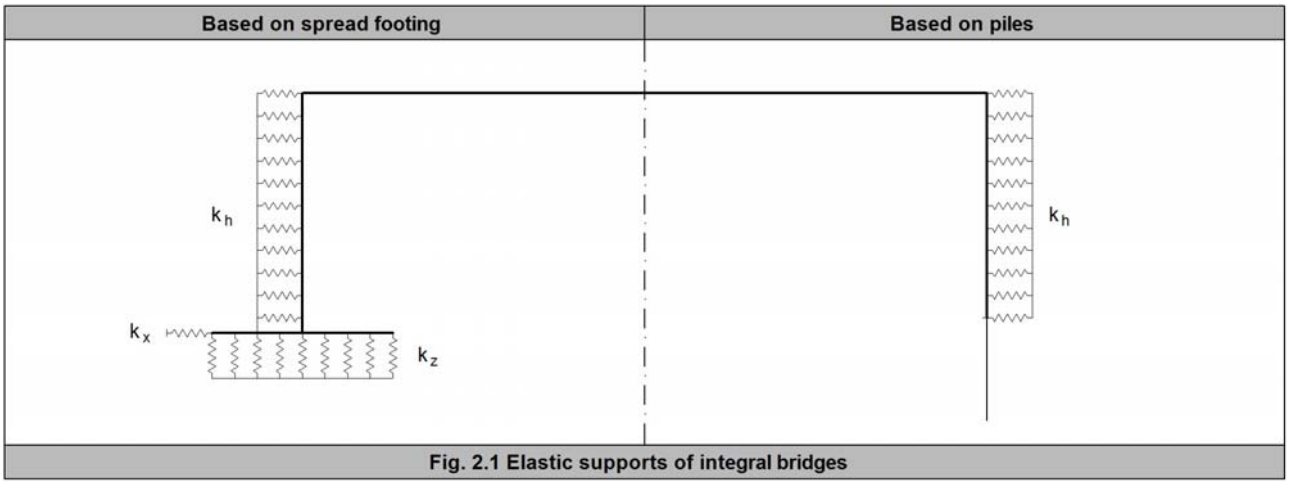

Fig. 2.1 Elastic supports of integral bridges

- k_h is the modulus of subgrade reaction on abutments in horizontal direction which represents passive earth resistance of the backfill induced by pushing of the abutment into the soil,
- k_z is modulus of subgrade reaction below spread footing in vertical direction which represents compressibility of the subsoil,
- k_x is modulus of subgrade reaction below spread footing in horizontal direction which represents the shear resistance of the footing bottom against the horizontal displacements.

The moduli of subgrade reaction k_h are calculated upon these parameters:

1) Height of the abutment,
2) Length of the superstructure, which affects displacements of the abutment due to thermal expansion,
3) Type of the soil in backfill.

Moduli of subgrade reaction k_z and k_x calculated using the method depend on these parameters:

1) Dimensions of the spread footing,
2) Vertical and horizontal stress in the footing bottom,
3) Type of the subsoil below the spread footing,
4) Groundwater level in the subsoil.

Types and parameters of soil, which are necessary for the calculation of moduli of subgrade reaction k_h, k_z and k_x, are summarized in Annex A. Annex A relates to soil classification described in [2].

Calculation of moduli of subgrade reaction on piles is not covered in the method. Another literature is to be used to determine them.

On the basis of calculated moduli of subgrade reaction k_h, k_z and k_x, it is possible to determine the stiffness of elastic soil springs supporting the substructure of the integral bridge[2.1]. The soil springs can be introduced into the structural model used for the practical design, see Figure 2.1.

Described method is applicable generally for a wide range of integral bridges. It can be used both for single-span and multi-span integral bridges with any type of superstructure, i.e. for the steel, composite, reinforced and prestressed concrete bridges. The reaction moduli k_h can be used for reinforced concrete abutments, where no significant bending deflections caused by horizontal earth pressures occur. Calculated values of the reaction moduli k_h are applicable to the abutments founded on the spread footings or piles.

Note 2.1: Soil is generally non-linear elastic-plastic material. If soil deformation occurs, this deformation has always elastic and plastic component. These components are difficult to separate, because the elastic and plastic deformations occur simultaneously. This behavior is comprehended in the presented method for calculation of reaction moduli k_h, k_z and k_x. Reaction moduli calculated according to this method include both elastic and plastic soil deformations and give a true picture of non-linear soil behavior. In the practical use of the method, the stiffnesses of the soil springs are determined from the calculated reaction moduli. These soil springs, which are used in the structural model of the bridge, are usually considered as linear. It means that the stiffness of the springs is constant and independent on the load magnitude. Despite this simplification of real elastic-plastic behavior of the soil, the use of the linear springs is considered being enough accurate to simulate the elastic support of the integral bridges. However, in many cases, it is appropriate to minimize the plastic deformations of the soil (for example the soil in the backfill) in the bridge design. Using this method, it is possible to calculate the measure of the plastic deformations by the way described in the notes 5.1 and 5.2. It gives designer information about the possible soil plasticity, which should be avoided.

3 CALCULATION OF REACTION MODULI k_h

This chapter deals with reaction moduli k_h on the abutments. General procedure of calculation of the distribution of reaction moduli k_h on the abutments is described.

3.1 Distributions of Reaction Moduli k_h on Abutment

Distribution of the reaction moduli k_h depends on the mode of displacement of the abutment into the backfill caused by the thermal expansion and other effects. The displacement is defined by these two parameters:

1) Horizontal displacement at the top of the abutment u_T,
2) Horizontal displacement at the bottom of the abutment u_B.

The distributions of the reaction moduli along the depth of the abutment are shown in Figure 3.1. At the horizontal axis, there are values of reaction moduli k_h, vertical axis represents the depths z under the surface.

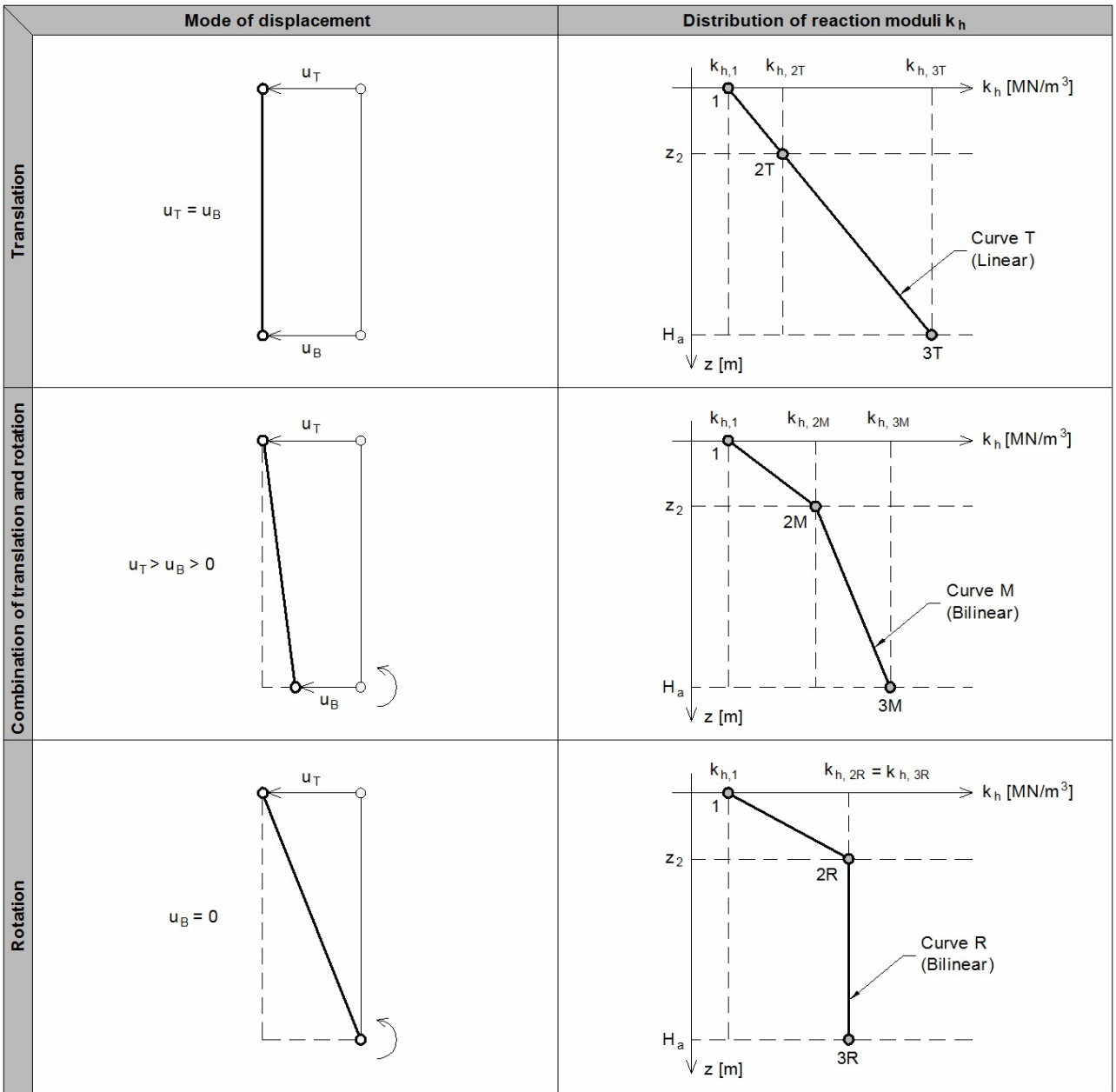

Fig. 3.1 Distributions of moduli of subgrade reaction on abutment

There are three different distributions of k_h depending on the displacement mode of the abutment:

1) **Translation of the abutment ($u_T = u_B$):** In this case, the distribution of the moduli k_h is described by linear **curve T**, which is defined by point 1 at the top of the abutment and by point 3T at the bottom of the abutment. Between the points 1 and 3T, there is an intermediate point 2T at depth z_2.

2) **Rotation of the abutment ($u_B = 0$):** In this case, the distribution of reaction moduli k_h is described by bilinear **curve R**, which is defined by points 1, 2R and 3R. Point 1 is identical with curve T, point 2R is at the same depth z_2 below the surface as point 2T. Point 3R is at the bottom of the abutment and is located vertically under point 2R.

3) **Combination of rotation and translation of the abutment ($u_T > u_B > 0$):** The distribution of reaction moduli k_h is described by bilinear **curve M**, located between curves T and R. Curve M is defined by points 1, 2M, and 3M. Point 1 is identical with curves T and R, point 2M is at the same depth z_2 as points 2T and 2R. The position of point 2M between points 2T and 2R can be determined by the linear interpolation according to the value u_B ranging between 0 and u_T. Point 3M is located at the bottom of the abutment. Its position between points 3T and 3R can be determined by the interpolation as well as by point 2M.

3.2 Definition of Points at Curves T, R and M

It is necessary to define points 1, 2R and 3T to determine curves T, R, and M for the particular case. Reaction moduli k_h of points 1, 2R and 3T, as well as depth z_2, have to be calculated. These values are calculated using following formulas:

$$k_h = \frac{A\,E_{ref}\,u_T}{10^4} + \frac{B\,E_{ref}}{10^2} + \frac{C\,u_T}{10^2} + D \qquad (3.1)$$

$$z_2 = \frac{A\,E_{ref}\,u_T}{10^4} + \frac{B\,E_{ref}}{10^2} + \frac{C\,u_T}{10^2} + D \qquad (3.2)$$

where:
- k_h is reaction modulus in MN/m^3 in the horizontal direction for appropriate point,
- z_2 depth of points 2R and 2T in meters,
- A to D factors for calculation of horizontal reaction moduli k_h on abutments, see Tables B.1 and B.2, Annex B,
- E_{ref} reference stiffness modulus of soil in the backfill in MPa in the drained and compacted state assuming $I_D > 0{,}75$,
- u_T horizontal displacement at the top of abutment in mm.

Factors A, B, C and D can be found for each point 1, 2R, 3T and depth z_2 in Tables B.1 and B.2 Annex B depending on the height of the abutment H_a and on the soil type (sand or gravel). Point 2T is located on the join of points 1 and 3T in depth z_2. Point 3R is located on the vertical under point 2R. Curves M for the combination of rotation and translation of the abutment can be allocated by interpolation between the relevant curves R and T. The calculation of the reaction moduli k_h and depths z of the points 1, 2T, 2R, 2M, 3T, 3R and 3M is summarized in Table 3.1.

Table 3.1 Points of the curves T, R and M		
Point	k_h [MN/m^3]	z [m]
1	$k_{h,1} = \frac{A_1 E_{ref} u_T}{10^4} + \frac{B_1 E_{ref}}{10^2} + \frac{C_1 u_T}{10^2} + D_1$ (3.3)	0
2T	$k_{h,2T} = k_{h,1} + \frac{(k_{h,3T} - k_{h,1}) z_2}{H_a}$ (3.4)	
2R	$k_{h,2R} = \frac{A_2 E_{ref} u_T}{10^4} + \frac{B_2 E_{ref}}{10^2} + \frac{C_2 u_T}{10^2} + D_2$ (3.5)	$z_2 = \frac{A_z E_{ref} u_T}{10^4} + \frac{B_z E_{ref}}{10^2} + \frac{C_z u_T}{10^2} + D_z$ (3.10)
2M	$k_{h,2M} = k_{h,2R} - \frac{(k_{h,2R} - k_{h,2T}) u_B}{u_T}$ (3.6)	
3T	$k_{h,3T} = \frac{A_3 E_{ref} u_T}{10^4} + \frac{B_3 E_{ref}}{10^2} + \frac{C_3 u_T}{10^2} + D_3$ (3.7)	
3R	$k_{h,3R} = k_{h,2R}$ (3.8)	H_a
3M	$k_{h,3M} = k_{h,3R} - \frac{(k_{h,3R} - k_{h,3T}) u_B}{u_T}$ (3.9)	
Factors A, B, C and D can be found for each point in Tables B.1 and B.2 Annex B. Reference stiffness modulus of soil E_{ref} in the drained state is appointed in [MPa]. Horizontal displacements u_T and u_B are appointed in [mm].		

3.3 Reaction Moduli k_h of Skewed Bridges

The method presented above is valid in case of straight bridges, where the displacement of the abutment is perpendicular to its back, see Figure 3.2a. By skewed bridges, it can be expected, that the displacement of the abutments caused by the thermal expansion and other effects occurs mostly in the longitudinal axis of the bridge, see Figure 3.2b. This displacement can be divided into two directions:

1) **Perpendicular to the abutment backside:** Resistance of the soil caused by this displacement can be considered as elastic soil springs expressed by moduli k_h. The displacements perpendicular to the backside of the abutment can be used to calculate moduli k_h according to paragraphs 3.1 and 3.2.

2) **Parallel with the abutment backside:** In case of this displacement, the resistance of the soil depends on the friction between the backside of the abutment and the backfill. The method presented above does not deal with this effect. If the skew of the bridge is less than 30°, the friction can be neglected. Otherwise, it should be considered, whether the friction has a significant effect for the interaction between the bridge structure and the backfill.

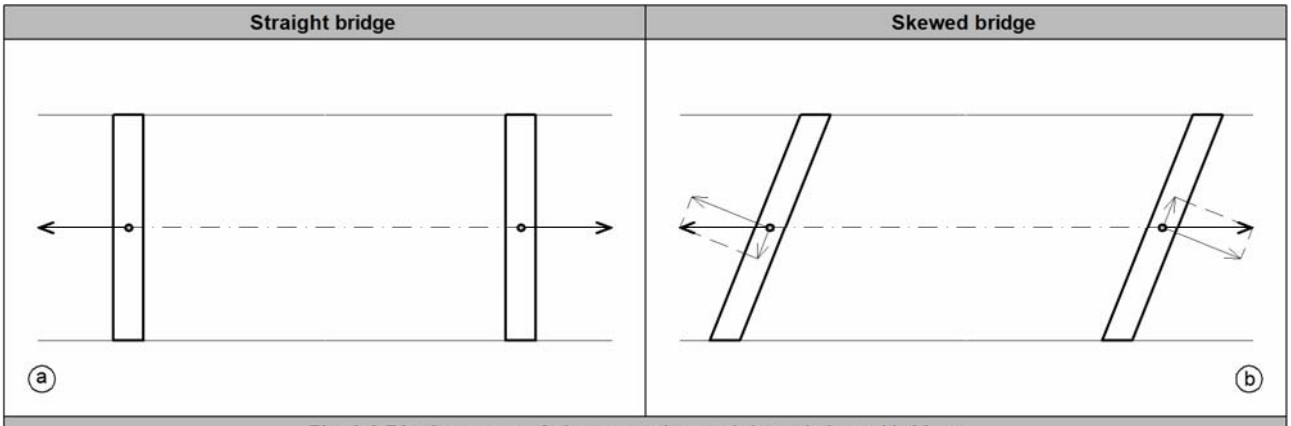

Fig. 3.2 Displacement of abutments by straight and skewed bridges

3.4 Validity and Application of the Method

Described method for calculation of moduli k_h is applicable under following assumptions:

1) **Superstructure of the integral bridge:** Described method is applicable to the all types of the superstructures, i.e. to the steel, composite, reinforced and prestressed concrete integral bridges.

2) **Span, number of spans and bridge length:** In the climatic conditions of the central Europe and other countries with the similar climate, the method is applicable to the bridges of the total length up to 130 m[3.1]. In countries, where maximal summer temperatures given by the actual standards are higher, the maximal bridge length is reduced to correspond with the condition of point 7, see below. The number of spans can be arbitrary.

3) **Skewed bridges:** The method can be used with the sufficient accuracy for the bridges with skew up to 30°, see paragraph 3.3. Otherwise, it should be considered, whether the skew has a significant effect for the interaction between the bridge structure and the backfill.

4) **Abutments:** The method was derived for rigid reinforced concrete abutments, where small deflections due to the passive earth pressure occur. The abutment height of ranges between 2 and 15 m.

5) **Foundation of the bridge:** The method can be used for bridges based on spread footings or piles.

6) **Soil in the backfill:** There are expected non-cohesive, non-frost susceptible sandy or gravely soils classified as SW-SC or GW-GC. The method is valid in the range of soil parameters listed in Annex A. There is also assumption, that the backfill is drained and compacted to the density index $I_D \geq 0{,}75$.

7) **Horizontal displacements of the abutments into the backfill:** Translation, rotation and their combination is expected. At the same time it is assumed, that the horizontal displacements at the top and at the bottom of the abutment u_t and u_b vary in the range 0-36 mm[3.1].

8) **Factors A, B, C and D** for points 1, 2R, 3T and depth z_2 are given in Tables B.1 and B.2, Annex B. For interjacent abutment heights, it is possible to interpolate in Tables B.1 and B.2.

9) **Horizontal displacement at the top of the abutment u_T** is appointed in mm. Despite points 2R and 3T are not at the top of the abutment, the horizontal displacement at the top of the abutment u_T is always appointed into formulas (3.1) to (3.10).

10) **Reference stiffness modulus E_{ref}** is appointed in MPa. If no accurate values of E_{ref} are available, it is possible to use the values given in Tables A.1 and A.2, Annex A.

In compliance with the above noted assumptions, the values of the reaction moduli k_h obtained from formulas in Table 3.1 are in MN/m^3. The way in which the method was derived is described in detail in [14].

Note 3.1: The method was derived for the displacement u_t and u_b ranging between 0 and 36mm (point 7). Assuming symmetrical expansion on the both bridge ends, maximal elongation of the bridge is $\Delta L = 72$ mm. According to [4], the maximal temperature $\Delta T_{N,\,exp}$ for the bridge elongation is considered 46°C for the steel bridges. In case of concrete and composite bridges, this value is lower. The total length L_{tot} of the bridge can be calculated from the formula $L_{tot} = \Delta L / (\alpha_t \, \Delta T_{N,\,exp}) = 0{,}072 / (12.10^{-6}. 46) = 130$ m. This implies the maximal length criterion of the bridge presented in the assumption point 2. This criterion does not take into the account other static or structural limits.

4 CALCULATION OF REACTION MODULI k_z AND k_x

This chapter describes calculation of reaction moduli k_z and k_x for the homogenous and stratified subsoil below the spread footing. The presented formulas are based on the assumption, that the distribution of the reaction moduli is uniform across the entire area of the footing bottom.

4.1 Vertical Reaction Moduli k_z for Homogenous Subsoil

Formula (4.1) for calculation of reaction moduli k_z is based on the assumption that the subsoil below the spread footing consist of one soil class only, whereas classification given in Annex A is used. Reaction modulus k_z is calculated as follows:

$$k_z = \left(\frac{K}{L + f_z} + M \right) \frac{E_{ref}}{N} W_z \tag{4.1}$$

where: k_z is reaction modulus in MN/m^3 in the vertical direction for the homogenous subsoil with the effect of groundwater,

K, L, M, N factors dependent on the footing dimensions and on the soil type, see Tables C.1- C.4, Annex C,

W_z factor reflecting the groundwater level, see Table E.1, Annex E,

E_{ref} reference stiffness modulus of the subsoil under drained conditions in MPa,

f_z vertical stress in the footing bottom in kN/m^2 considered as an average uniform value across the whole area of the footing bottom.

4.2 Horizontal Reaction Moduli k_x for Homogenous Subsoil

Formula (4.2) for calculation of reaction moduli k_x is based on the assumption that the subsoil below the spread footing consist of one soil class only whereas classification given in Annex A is used. Reaction moduli k_x is calculated as follows:

$$k_x = \left(\frac{P f_x f_z - Q f_x}{R} - S f_z + T \right) \frac{G_{ref}}{U} W_x \tag{4.2}$$

where: k_z is reaction modulus in MN/m^3 in the horizontal direction for the homogenous subsoil with the effect of groundwater,

P to U factors dependent on the footing dimensions and on the soil type, see Tables D.1 - D.4, Annex D,

W_x factor reflecting the groundwater level, see Table E.1, Annex E,

G_{ref} reference shear stiffness modulus of the subsoil under drained conditions in MPa,

f_z, f_x vertical and horizontal stresses in the footing bottom in kN/m^2 considered as an average uniform value across the whole area of the footing bottom.

In case of the fine-grained soils classified as F3 to F6, the effect of the horizontal stress f_x in footing bottom is negligible, as far as modulus k_x is concerned. Formula (4.2) can be reduced to the form:

$$k_x = \left(-S f_z + T \right) \frac{G_{ref}}{U} W_x \tag{4.3}$$

4.3 Vertical and Horizontal Reaction Moduli for Layered Subsoil

The formulas shown in paragraphs 4.1 and 4.2 are valid assuming that the subsoil below the footing is homogenous. However, cases with layered subsoil occur in practice. This paragraph describes the method how to calculate vertical and horizontal reaction moduli k_{zs} and k_{xs} for the layered subsoil below the spread footing. The calculation is based on the general principle, that the reciprocal value of the reaction modulus of the layered subsoil is equal to the sum of the reciprocal values of reaction moduli of the particular layers. If the layered subsoil consists of n layers, the total reaction moduli k_{zs} and k_{xs} of the layered subsoil can be calculated as follows:

$$k_{zs} = \left(\sum_{i=1}^{n} \frac{1}{k_{zi}} \right)^{-1} \tag{4.4}$$

$$k_{xs} = \left(\sum_{i=1}^{n} \frac{1}{k_{xi}} \right)^{-1} \tag{4.5}$$

where: k_{zi}, k_{xi} are vertical and horizontal reaction moduli of the particular i^{th} layer of the subsoil.

Reaction moduli of the particular layers k_{zi} and k_{xi} can be calculated according to following formulas:

$$k_{zi} = \frac{k_z}{u_{rTz} - u_{rBz}} \tag{4.6}$$

$$k_{xi} = \frac{k_x}{u_{rTx} - u_{rBx}} \tag{4.7}$$

where: k_z, k_x are vertical and horizontal reaction moduli calculated according to formulas (4.1) to (4.3) supposing homogenous subsoil,

u_{rTz}, u_{rTx} relative vertical and horizontal displacements at the top of the particular i^{th} layer (point T, Figure 4.1),

u_{rBz}, u_{rBx} relative vertical and horizontal displacements at the bottom of the particular i^{th} layer (point B, Figure 4.1).

Relative displacements u_{rTz}, u_{rTx}, u_{rBz} and u_{rBx} can be obtained from the graph in Figure 4.1. This graph shows the relationship between relative depth z_r and relative displacement u_r. If the top of the particular i^{th} layer is in the depth z_T (point T) and the bottom in the depth z_B (point B), relative depths z_{rT} and z_{rB} are calculated:

$$z_{rT} = \frac{z_T}{H_s} \tag{4.8}$$

$$z_{rB} = \frac{z_B}{H_s} \tag{4.9}$$

where: z_T, z_B are the depths of points T and B at the top and at the bottom of the i^{th} layer,

H_s depth of compressible subsoil, see the Table F.1, Annex F.

The depth of the compressible subsoil H_s depends on the type of soil, on the value of vertical stress in the footing bottom and on the dimensions of the footing. Values of H_s can be found in Table F.1, Annex F. H_s represents the compressible part of subsoil below the footing, where significant deformations caused by the footing load occur.

Relative displacements u_{rTz}, u_{rBz}, u_{rTx} and u_{rBx} can be obtained from the graph in Figure 4.1 upon depths z_{rT} and z_{rB}. Relative displacements u_{rTz} and u_{rBz} in the vertical direction can be obtained from the branch of the graph for vertical direction, while relative displacements u_{rTx} and u_{rBx} in the horizontal direction can be obtained from the branch for horizontal direction.

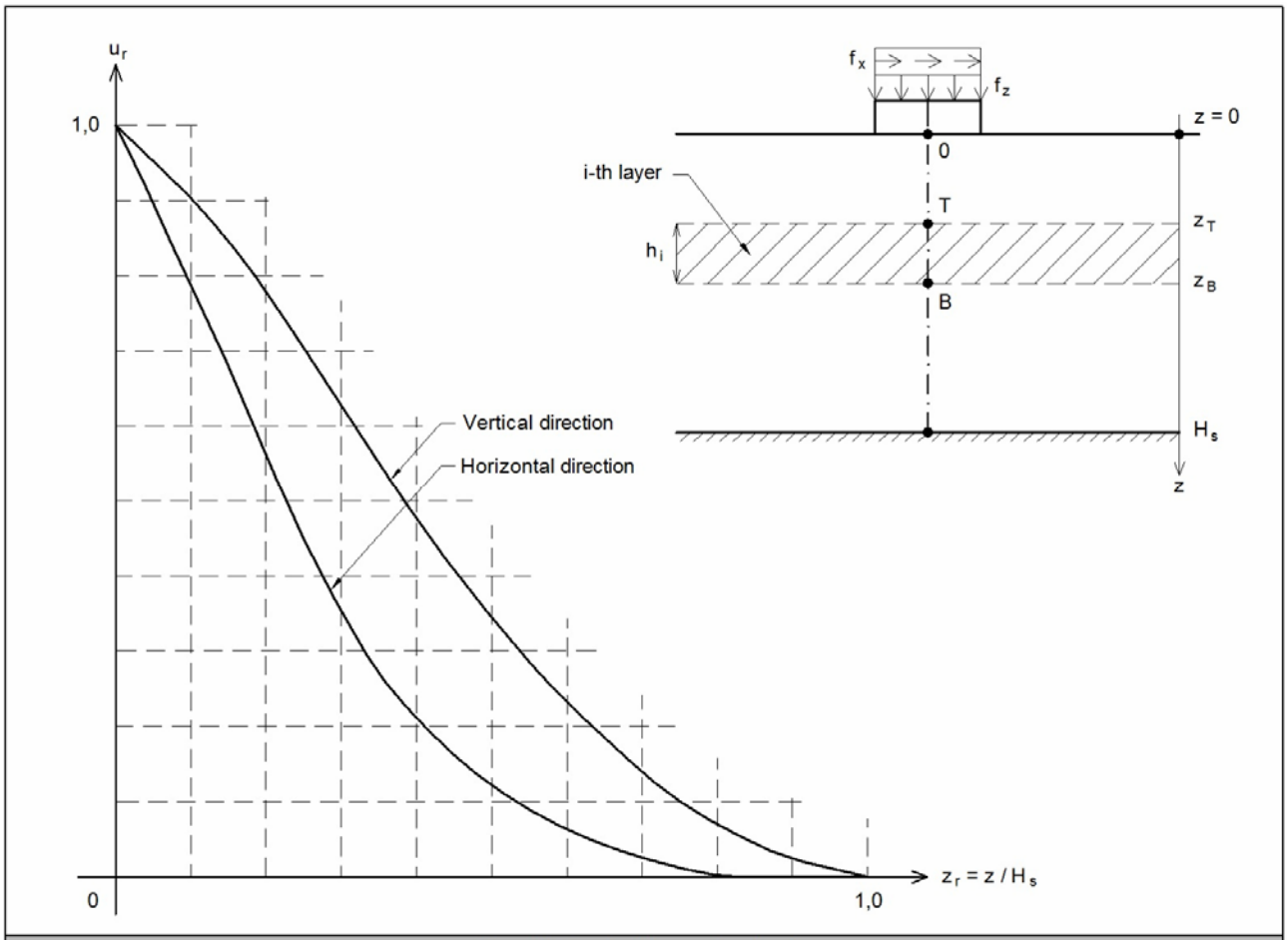

Fig. 4.1 Graph of layered subsoil

4.4 Moduli k_z and k_x of Skewed Bridges

The calculation method of the reaction moduli k_z and k_x was developed for straight bridges with a rectangular spread footing with the width B_f and the length L_f. However, the method can be also used for bridges with skew up to 30°. If the spread foundation has the rhomboid plan view, it can be substituted by the rectangular foundation (Figure 4.2) for the purposes of calculation of moduli k_z and k_x.

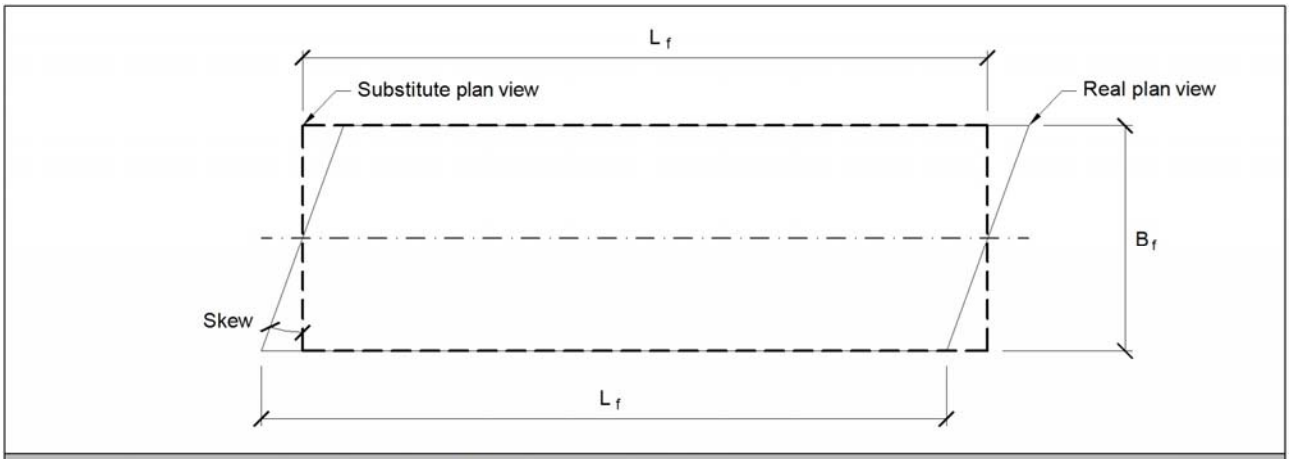

Fig. 4.2 Substitute plan view for skewed bridges

4.5 Validity and Application of the Method

Described method for calculation of moduli k_z, k_x, k_{zs} and k_{xs} is applicable under following assumptions:

1) **Dimensions of the foundations:** between 3x6 and 8x32 $m^{4.1}$.

2) **Skewed bridges:** Above-described method can be used with the sufficient accuracy for the bridges with skew up to 30°, see paragraph 4.4. Otherwise, it is necessary to consider whether the skew of bridge has significant effect on the values of the reaction moduli k_z and k_x.

3) **Soil in subsoil:** Sandy soil classified as SW-SC, gravelly soil classified as GW-GC and fine-grained soil classified as MG-CI are assumed. The method is applicable in the range of soil parameters given in Annex A. It is assumed that the soil in the subsoil is compacted to the value of the relative density $I_D \geq 0{,}75$. In case of the fine-grained soil, the firm consistency is assumed.

4) **Groundwater level:** The effect of the groundwater is considered using factors W_z and W_x. Factors W_z and W_x are summarized in Table E.1, Annex E.

5) **Vertical and horizontal stress f_z and f_x in the footing bottom:** Vertical stress f_z in the footing bottom is for particular soils limited by values of $f_{z,\,lim}$ listed in Table G.1, Annex G. Similarly, horizontal stress f_x is limited by the values of $f_{x,\,lim}$. The values of $f_{x,\,lim}$ are also summarized in Table G.1. Vertical and horizontal stresses f_z and f_x are used in kN/m^2 in formulas 4.1 to 4.3 and their values are assumed constant across the whole area of footing bottom.

6) **Factors K, L, M, N and P, Q, R, S, T, U** are listed in tables C.1 to C.4 of Annex C and in Tables D.1 to D.4 of Annex D. In case of the interjacent values of footing dimensions, it is possible to interpolate in tables. Similarly, it is possible to interpolate between the particular soil classes. In case of the fine-

grained soils, the factors for the effective parameters (Tables C.3 and D.3) are used in case of the long-term loading effects. In case of the short-term effects, the total parameters (Tables C.4 and D.4) are used.

7) **Reference stiffness moduli E_{ref} and G_{ref}** are used in MPa. If no accurate values of E_{ref} and G_{ref} are available, it is possible to use the values given in Tables A.1 to A.3 of Annex A. In case of fine-grained soils, the total parameters are used for short-term loading effects, the effective parameters are used for the long-term loading, see Table A.3 of Annex A.

In compliance with the above noted assumptions, the values of the reaction moduli k_z, k_x, k_{zs} and k_{xs} obtained from formulas (4.1) to (4.7) are in MN/m^3. The way in which the method was derived is described in detail in [14].

Note 4.1: The method was derived for footing dimensions in the range of 3x6 to 8x32 m, and consequently the factors K, L, M, N and P, Q, R, S, T, U were determined. This criterion does not take into the account other static or structural limits.

5 EXAMPLES

5.1 Example 1

Determine the distribution of the reaction moduli k_h on an abutment. The geometry of the abutment is shown in Figure 5.1. The height of the abutment H_a = 7,5 m, the backfill is provided by dense sandy material with stiffness modulus E_{ref} = 40 MPa. The horizontal displacement at the top of the abutment u_T = 6,0 mm, the horizontal displacement at the bottom of the abutment u_B = 3,0 mm.

The displacement of the abutment is a combination of translation and rotation. In this case, the distribution of reaction moduli is defined by bilinear curve M, as shown in Figure 3.1. The bilinear curve M is located between linear curve T, where $u_T = u_B$ = 6,0 mm (translation), and bilinear curve R, where u_T = 6,0 mm and u_B = 0,0 mm (rotation). The distribution of reaction moduli k_h is determined in the following steps:

1) Determination of linear curve T, supposing $u_T = u_B$ = 6,0 mm, representing horizontal translation of the abutment.
2) Determination of bilinear curve R, supposing u_T = 6,0 mm and u_B = 0,0 mm, representing rotation of the abutment.
3) Determination of final intermediate bilinear curve M, where u_T = 6,0 mm and u_B = 3,0 mm, representing combination of translation and rotation of the abutment.

1. Linear Curve T

To determine curve T, see Figure 3.1, it is necessary to calculate values of the reaction moduli $k_{h,1}$, $k_{h,2T}$, $k_{h,3T}$ and depth z_2. Formulas given in Table 3.1 are used. Factors A, B, C and D are obtained from Table B.1, Annex B. The values of the factors are interpolated between the values for abutment heights H_a 7 and 8 m.

$$k_{h,1} = \frac{A_1 E_{ref} u_T}{10^4} + \frac{B_1 E_{ref}}{10^2} + \frac{C_1 u_T}{10^2} + D_1 = \frac{-6{,}0 \,.\, 40 \,.\, 6{,}0}{10^4} + \frac{4{,}45 \,.\, 40}{10^2} + \frac{0{,}0 \,.\, 6{,}0}{10^2} + 0{,}0 = 1{,}6 \text{ MN/m}^3$$

$$k_{h,3T} = \frac{A_3 E_{ref} u_T}{10^4} + \frac{B_3 E_{ref}}{10^2} + \frac{C_3 u_T}{10^2} + D_3 = \frac{-16{,}0 \,.\, 40 \,.\, 6{,}0}{10^4} + \frac{16{,}5 \,.\, 40}{10^2} + \frac{1{,}05 \,.\, 6{,}0}{10^2} + 0{,}55 = 6{,}8 \text{ MN/m}^3$$

$$z_2 = \frac{A_z E_{ref} u_T}{10^4} + \frac{B_z E_{ref}}{10^2} + \frac{C_z u_T}{10^2} + D_z = \frac{1{,}25 \,.\, 40 \,.\, 6{,}0}{10^4} + \frac{0{,}25 \,.\, 40}{10^2} + \frac{1{,}4 \,.\, 6{,}0}{10^2} + 0{,}7 = 0{,}9 \text{ m}$$

$$k_{h,2T} = k_{h,1} + \frac{(k_{h,3T} - k_{h,1})\, z_2}{H_a} = 1{,}6 + \frac{(6{,}8 - 1{,}6)\, 0{,}9}{7{,}5} = 2{,}2 \text{ MN/m}^3$$

2. Bilinear Curve R

To determine curve R, see Figure 3.1, it is necessary to calculate values of the reaction moduli $k_{h,1}$, $k_{h,2R}$, $k_{h,3R}$ and depth z_2 according to formulas in Table 3.1. As well as by curve T, factors A, B, C and D are obtained from Table B.1 and interpolated.

$k_{h,1} = 1{,}6 \text{ MN/m}^3$ (See linear curve T)

$$k_{h,2R} = \frac{A_2\, E_{ref}\, u_t}{10^4} + \frac{B_2\, E_{ref}}{10^2} + \frac{C_2\, u_t}{10^2} + D_2 = \frac{-6{,}2 \,.\, 40 \,.\, 6{,}0}{10^4} + \frac{14{,}9 \,.\, 40}{10^2} + \frac{0{,}0 \,.\, 6{,}0}{10^2} + 0{,}75 = 6{,}6\ \mathrm{MN/m^3}$$

$$k_{h,3R} = k_{h,2R} = 6{,}6\ \mathrm{MN/m^3}$$

$z_2 = 0{,}9\ \mathrm{m}$ (See linear curve T)

3. Bilinear Curve M

To determine curve M, see Figure 3.1, it is necessary to calculate the values of the reaction moduli $k_{h,1}$, $k_{h,2M}$, $k_{h,3M}$ and depth z_2. These values are interpolated between curves T and R according to formulas in Table 3.1.

$k_{h,1} = 1{,}6\ \mathrm{MN/m^3}$ (See linear curve T)

$$k_{h,2M} = k_{h,2R} - \frac{(k_{h,2R} - k_{h,2T})\, u_B}{u_T} = 6{,}6 - \frac{(6{,}6 - 2{,}3)\, 3{,}0}{6{,}0} = 4{,}4\ \mathrm{MN/m^3}$$

$$k_{h,3M} = k_{h,3R} - \frac{(k_{h,3R} - k_{h,3T})\, u_B}{u_T} = 6{,}6 - \frac{(6{,}6 - 6{,}8)\, 3{,}0}{6{,}0} = 6{,}7\ \mathrm{MN/m^3}$$

$z_2 = 0{,}9\ \mathrm{m}$ (See linear curve T)

The final distribution of reaction moduli k_h on the abutment is shown in Figure 5.1 (curve M)[5.1]. In addition, curves T and R are displayed.

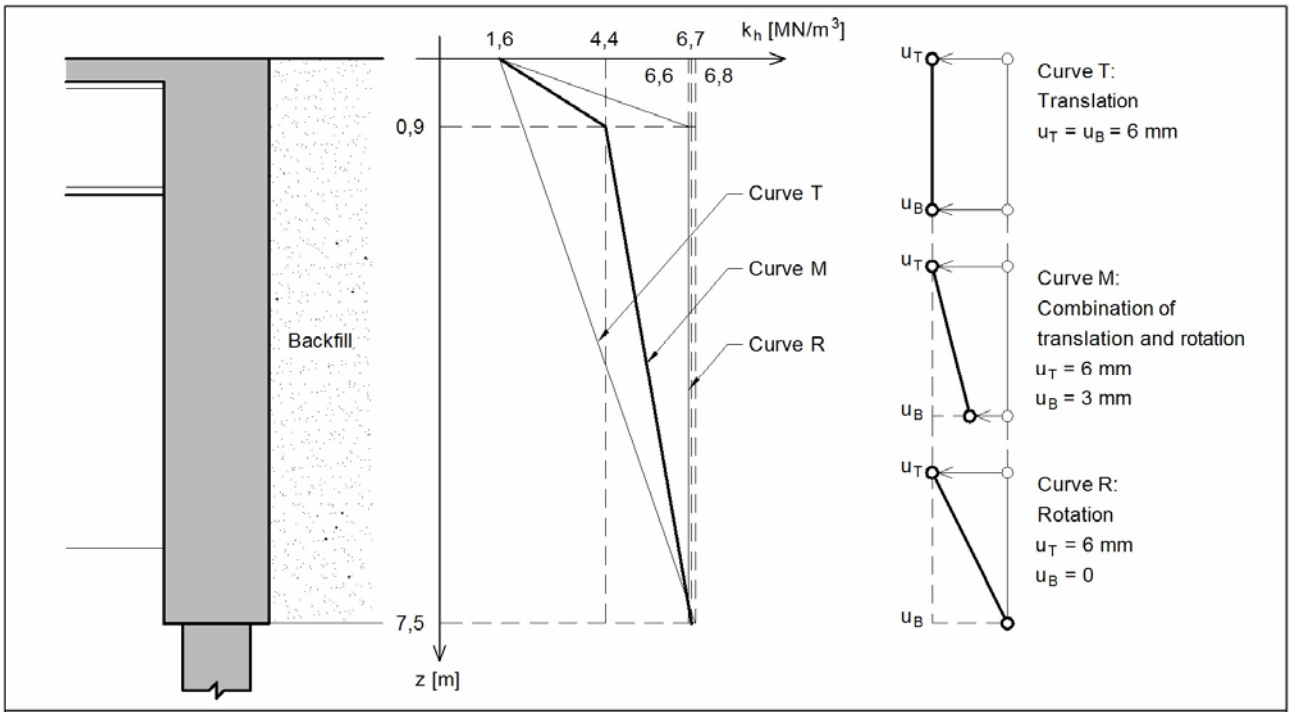

Fig. 5.1 Distribution of reaction moduli on abutment

Note 5.1: Deformations of the backfill due to abutment displacement consist of elastic and plastic component, see Note 2.1. However, the aim of the practical design of the backfill is to minimize plastic deformation due to the cyclic movements of the abutment. The reaction moduli k_h calculated by this method take into the account the elastic-plastic behavior of the soil. The plastic component of the deformation can be determined by this method in the following way: The distribution of k_h can be calculated for the required translations u_t and u_b first. The distribution of k_h can be then calculated for other values of translations, for example, for $u_T/2$ and $u_B/2$. If the distributions of k_h are similar in both cases, we conclude that the elastic behavior of the backfill prevails. If the distributions differ significantly, it indicates plastic behavior of the backfill. Any changes in the design of the substructure should be considered in this case.

5.2 Example 2

Calculate vertical and horizontal reaction moduli k_{zs} and k_{xs} of a rectangular spread footing. The geometry of the footing and the subsoil are shown in Figure 5.2. Width of the footing B_f = 5,0 m and length L_f = 12,0 m. There is a vertical normal stress f_z = 200 kN/m^2 and a horizontal shear stress f_x = 15 kN/m^2 in the footing bottom. The subsoil below the footing consists of two layers: 1) layer of sandy soil classified as SF with thickness of 4,0 m, Stiffness modulus E_{ref} = 21,0 MPa and shear stiffness modulus G_{ref} = 8,0 MPa, 2) layer of gravely soil classified as GF with thickness of 5,0 m, stiffness modulus E_{ref} = 95,0 MPa and shear stiffness modulus G_{ref} = 38,0 MPa. The groundwater level is 5,0 m below the terrain.

To calculate the reaction moduli, the subsoil is divided into three layers:

1) The layer of soil classified as SF, thickness 4,0 m (layer 1),
2) The layer of soil classified as GF above the groundwater level, thickness 1,0 m (layer 2),
3) The layer of soil classified as G3 below the groundwater level, thickness 4,0 m (layer 3).

The reaction moduli k_{zs} and k_{xs} are calculated in four steps. In the first three steps, the partial reaction moduli k_{zi} and k_{xi} of each layer are calculated. In the fourth step, the total reaction moduli k_{zs} and k_{xs} is determined.

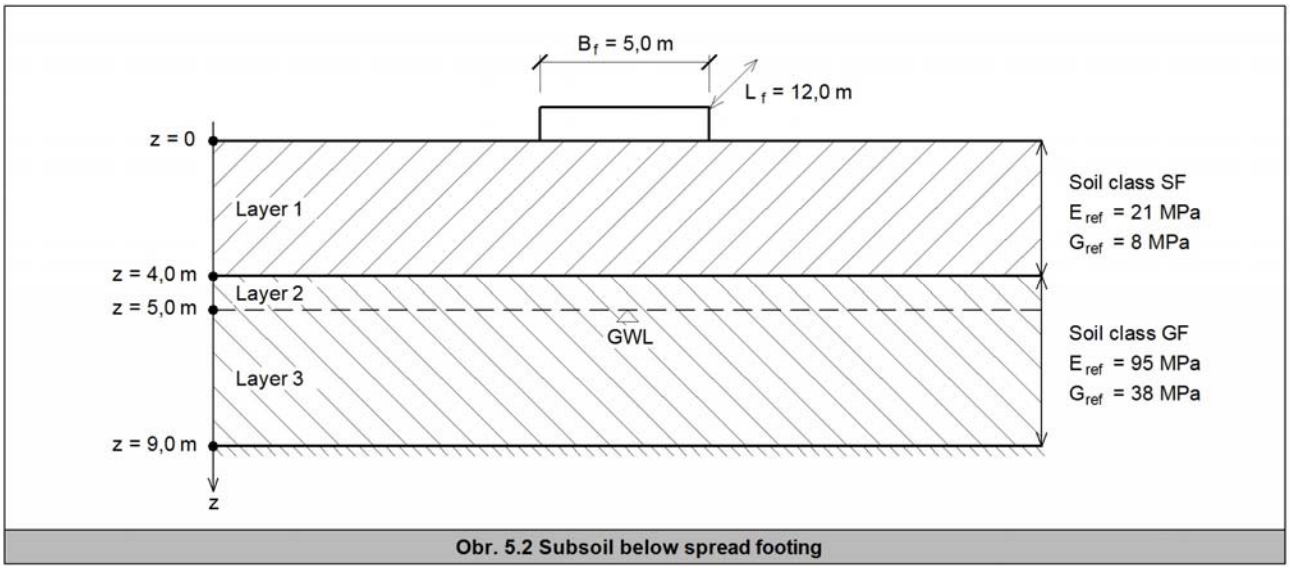

Obr. 5.2 Subsoil below spread footing

1. Layer 1

First, reaction moduli k_z and k_x are calculated using formulas (4.1) and (4.2), supposing homogenous subsoil consisting of soil classified as SF only. Factors K, L, M, N are obtained from Tables C.1 and C.2, Annex C. The factors are interpolated according to width B_f and length L_f. In case of footing dimensions 5x12 m, the final interpolated factors are:

K = 1204,0 L = 36,0 M = 1,66 N = 21,0

Factor W_z can be obtained from Table E.1, Annex E. Layer 1 is above the groundwater level, it follows:

W_z = 1,00

Putting all factors to formula (4.1), we get:

$$k_z = \left(\frac{K}{L + f_z} + M \right) \frac{E_{ref}}{N} W_z = \left(\frac{1204,0}{36,0 + 200} + 1,66 \right) \frac{21,0}{21,0} \; 0,95 = 6,4 \text{ MN/m}^3$$

Factors P, Q, R, S, T, U are obtained by interpolation in Table D.1, Annex D. In case of footing dimensions 5x12 m, the final interpolated factors are:

P = 0,0055 Q = 2,9 R = 50,0 S = 0,0082 T = 6,7 U = 8,1

Factor W_x is obtained from Table E.1, Annex E. Layer 1 is above the groundwater level, it follows:

$W_x = 1,0$

Putting all factors to formula (4.2), we get:

$$k_x = \left(\frac{P\, f_x\, f_z - Q\, f_x}{R} - S\, f_z + T \right) \frac{G_{ref}}{U} W_x = \left(\frac{0,0055 \,.\, 15 \,.\, 200 - 2,9 \,.\, 15}{50,0} - 0,0082 \,.\, 200 + 6,7 \right) \frac{8,0}{8,1} 1,0 =$$

$$= 4,5 \text{ MN/m}^3$$

Depth of the compressible subsoil H_s is obtained by interpolation in Table F.1, Annex F. Subsoil consisting of soil classified as SF is assumed. In case of footing dimensions 5x12 m and vertical stress in the footing bottom $f_z = 200$ kN/m^2 the final interpolated value is:

$H_s = 7,2$ m

Layer 1 is 4,0 m depth and is situated from 0 to 4 m below the footing bottom. It follows:

$z_T = 0,0$ m $z_B = 4,0$ m

Using formulas (4.8) and (4.9), we calculate relative depths z_{rT} and z_{rB} at the top and at the bottom of layer 1:

$$z_{rT} = \frac{z_T}{H_s} = \frac{0,0}{7,2} = 0,0 \qquad z_{rB} = \frac{z_B}{H_s} = \frac{4,0}{7,2} = 0,56$$

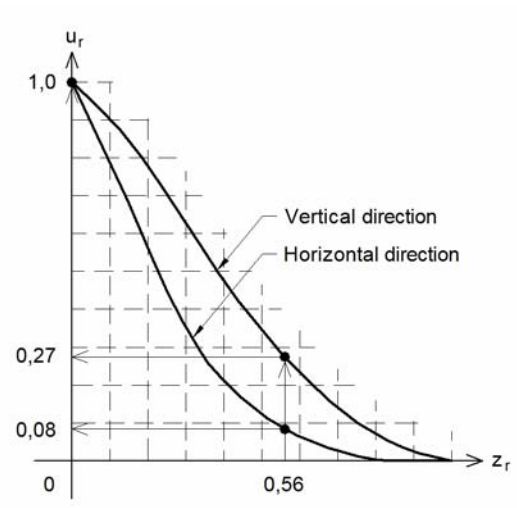

Using the graph of the layered subsoil (Figure 4.1) and above calculated relative depths z_{rT} and z_{rB}, we obtain relative displacements at the top and at the bottom of layer 1:

$u_{rTz} = 1,0$ $u_{rBz} = 0,27$ $u_{rTx} = 1,0$ $u_{rBx} = 0,08$

Putting in formulas (4.6) and (4.7), horizontal and vertical reaction moduli of layer 1 are calculated:

$$k_{z1} = \frac{k_z}{u_{rTz} - u_{rBz}} = \frac{6,4}{1,0 - 0,27} = 8,8 \text{ MN/m}^3$$

$$k_{x1} = \frac{k_x}{u_{rTx} - u_{rBx}} = \frac{4,5}{1,0 - 0,08} = 4,9 \text{ MN/m}^3$$

2. Layer 2

In case of layer 2, the calculation is analogous to the calculation of layer 1. Factors K, L, M, N can be determined by interpolation in Table C.2, factor W_z can be found in Table E.1:

K = 7108,0 L = 81,7 M = 7,0 N = 95,0 W_z = 1,00

$$k_z = \left(\frac{K}{L + f_z} + M \right) \frac{E_{ref}}{N} W_z = \left(\frac{7108,0}{81,7 + 200} + 7,0 \right) \frac{95,0}{95,0} \; 0,95 = 30,6 \text{ MN/m}^3$$

Similarly, an analogous way is proceeded in case of factors P, Q, R, S, T, U, W_x and modulus k_x.

P = 0,0122 Q = 12,2 R = 100,0 S = 0,0158 T = 25,3 U = 38,0 W_x = 1,0

$$k_x = \left(\frac{P f_x f_z - Q f_x}{R} - S f_z + T \right) \frac{G_{ref}}{U} W_x = \left(\frac{0,0122 . 15 . 200 - 12,2 . 15}{100,0} - 0,0158 . 200 + 25,3 \right) \frac{38,0}{38,0} 1,0 =$$

$$= 20,7 \text{ MN/m}^3$$

While determining depth H_s, homogenous subsoil consisting of soil classified as GF is assumed. H_s is obtained by interpolation in Table F.1:

H_s = 6,6 m

Layer 2 is 1,0 m depth and is situated from 4 to 5 m below the footing bottom. It follows:

z_T = 4,0 m z_B = 5,0 m

Using formulas (4.8) and (4.9), we calculate relative depths z_{rT} and z_{rB} at the top and at the bottom of layer 2:

$$z_{rT} = \frac{z_T}{H_s} = \frac{4,0}{6,6} = 0,61 \qquad z_{rB} = \frac{z_B}{H_s} = \frac{5,0}{6,6} = 0,76$$

Using the graph of the layered subsoil, we get:

u_{rTz} = 0,22 u_{rBz} = 0,09 u_{rTx} = 0,06 u_{rBx} = 0,01

Putting in formulas (4.6) and (4.7), horizontal and vertical reaction moduli of layer 2 are calculated:

$$k_{z2} = \frac{k_z}{u_{rTz} - u_{rBz}} = \frac{32,2}{0,22 - 0,09} = 247,7 \text{ MN/m}^3$$

$$k_{x2} = \frac{k_x}{u_{rTx} - u_{rBx}} = \frac{20,7}{0,06 - 0,01} = 414,0 \text{ MN/m}^3$$

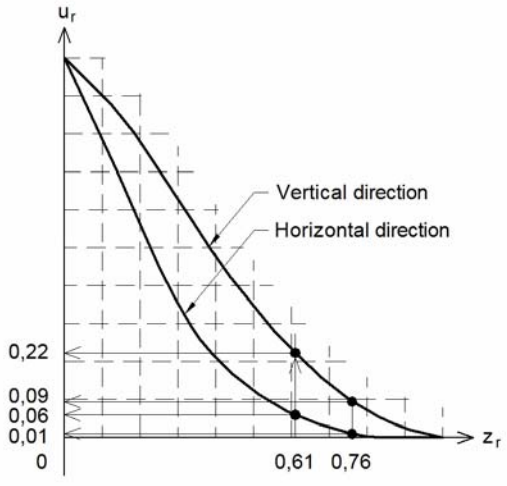

3. Layer 3

Calculation of layer 3 is analogous to layers 1 and 2. Factors K, L, M, N and P, Q, R, S, T, U are equal to the factors by layer 2. Layer 3 is below groundwater level. From Table E.1 follows:

W_z = 0,75 W_x = 0,80

$$k_z = \left(\frac{K}{L + f_z} + M \right) \frac{E_{ref}}{N} W_z = \left(\frac{7108,0}{81,7 + 200} + 7,0 \right) \frac{95,0}{95,0} \; 0,75 = 24,2 \text{ MN/m}^3$$

$$k_x = \left(\frac{P f_x f_z - Q f_x}{R} - S f_z + T \right) \frac{G_{ref}}{U} W_x = \left(\frac{0,0122 . 15 . 200 - 12,2 . 15}{100,0} - 0,0158 . 200 + 25,3 \right) \frac{38,0}{38,0} 0,80 =$$

$$= 16,5 \text{ MN/m}^3$$

The depth of the compressible subsoil is equal to layer 2, i.e. H_s = 6,6 m. Layer 3 is 4,0 m depth and is situated from 5 to 9 m below the footing bottom. It follows:

z_T = 5,0 m z_B = 9,0 m

The bottom of layer 3 is in the depth z_B = 9,0 m. It is more than the depth of the compressible subsoil H_s = 6,6 m, where the significant deformations occur. It means, that a part of layer 3 is in the incompressible area. Therefore, only the 6,6 m depth compressible part is considered in the calculation, i.e. z_B = 6,6 m.

$$z_{rT} = \frac{z_T}{H_s} = \frac{5,0}{6,6} = 0,76 \qquad z_{rB} = \frac{z_B}{H_s} = \frac{6,6}{6,6} = 1,0$$

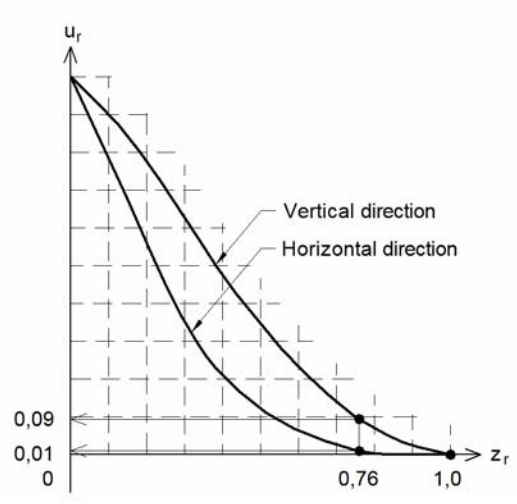

Using the graph of the layered subsoil, we get:

u_{rTz} = 0,09 u_{rBz} = 0,0 u_{rTx} = 0,01 u_{rBx} = 0,0

Putting in formulas (4.6) and (4.7), horizontal and vertical reaction moduli of layer 3 are calculated:

$$k_{z3} = \frac{k_z}{u_{rTz} - u_{rBz}} = \frac{24,2}{0,09 - 0,0} = 268,9 \text{ MN/m}^3$$

$$k_{x3} = \frac{k_x}{u_{rTx} - u_{rBx}} = \frac{16,5}{0,01 - 0,0} = 1650,0 \text{ MN/m}^3$$

4. Total Reaction Moduli

The total reaction moduli for layered subsoil k_{zs} and k_{xs} are calculated using formulas (4.4) and (4.5)[5.2]:

$$k_{zs} = \left(\sum_{i=1}^{n} \frac{1}{k_{zi}} \right)^{-1} = \left(\frac{1}{9,3} + \frac{1}{247,7} + \frac{1}{268,9} \right)^{-1} = 8,7 \text{ MN/m}^3$$

$$k_{xs} = \left(\sum_{i=1}^{n} \frac{1}{k_{xi}} \right)^{-1} = \left(\frac{1}{4,9} + \frac{1}{414,0} + \frac{1}{1650,0} \right)^{-1} = 4,8 \text{ MN/m}^3$$

Note 5.2: Deformations of the soil below the spread footing consist of the elastic and plastic components, see the Note 2.1. In some cases, reduction of plastic deformations caused by the vertical and horizontal loading of the footing is required. Reaction moduli k_z and k_x calculated by this method take into the account elastic-plastic behavior of the soil. The plastic component of the deformation can be determined by this method in the following way: First, reaction moduli k_z and k_x are calculated for the required stress in the footing bottom f_z and f_x. Second, the reaction moduli can than be determined for another stress, for example for $f_z/2$ and $f_x/2$. If the values of reaction moduli are similar in both cases, we conclude that the elastic behavior of the subsoil prevails. If the moduli differ significantly, it indicates plastic behavior of the subsoil.

5.3 Example 3

This example deals with the design of a single span road integral bridge with composite steel and concrete superstructure, see Figure 5.3. The bridge is straight with 2% longitudinal slope. The span of the bridge is 36 m, the height of the abutments is 10 m. The bridge is founded on the 5 m wide spread footings. The superstructure consists of 4 steel girders and of 12 m wide reinforced concrete slab. The spacing of steel girders is 3 m. All girders are identical. The distribution of reinforcement in the deck displayed in Figure 5.3 is constant across the whole width of the slab. The backfill behind the abutments is provided by dense sandy material classified as SP. There is 9 m depth layer of the compact SF sandy soil below the footing. Below this layer, there is incompressible bedrock. The groundwater level is 7 m below the footing bottom.

Determine:

- The distribution of the reaction moduli k_h on the abutment,
- Reaction moduli k_z and k_x of the subsoil below the spread footing,
- Stiffness of the soil springs supporting the integral bridge, which will be used in the structural model.

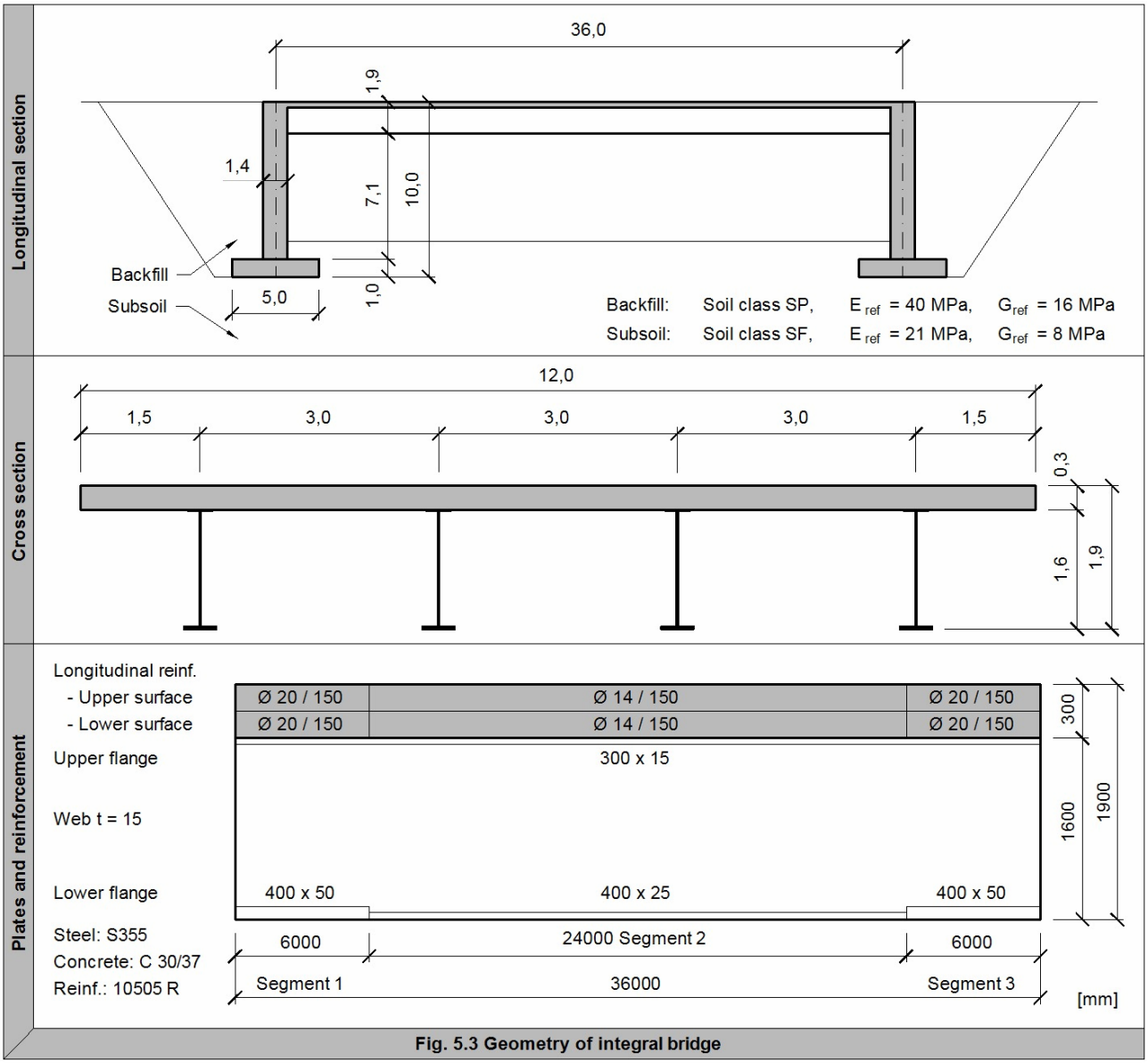

Fig. 5.3 Geometry of integral bridge

The solution is divided into three parts:

1) Definition of the structural model of the integral bridge based on the given geometry,

2) Determination of the crucial actons for calculation of the reaction moduli k_h, k_z and k_x,

3) Calculation of the reaction moduli k_h, k_z and k_x and of the stiffness K_h, K_z and K_x of the soil springs.

1. Structural Model of the Integral Bridge

The structural model consists of the superstructure and the substructure, because these parts interact together. Since the connection between the superstructure and the substructure is rigid, a frame corner is provided in the structural model. Surrounding soil is considered as distributed soil springs situated to the components of the substructure.

The planar structural model shown in Figure 5.4 is sufficient to determine the reaction moduli k_h, k_z and k_x. The planar model represents a longitudinal cut-out the bridge. The cut-out is 3 m wide and consists of:

- Member of the superstructure with the cross-section according to Figure 5.5a,
- Members of the abutments and footings with the cross-sections according to Figures 5.5b and 5.5c,
- Distributed linear springs with the stiffness K_h placed on the abutments, see Figure 5.4,
- Distributed linear springs with the stiffness K_z in the vertical direction and the stiffnesses K_x in the horizontal direction placed on the spread footings, see Figure 5.4.

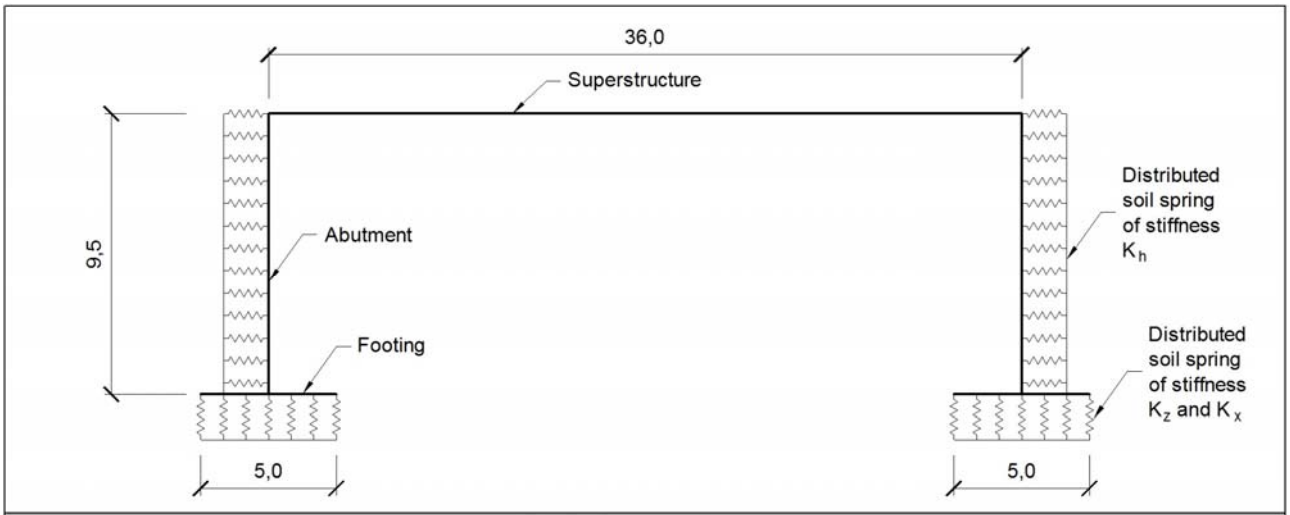

Fig. 5.4 Structural model

Superstructure

The cross-section of the superstructure is shown in Figure 5.5a. It consists of the steel girder made of the steel S355 and of the concrete slab made of the concrete C30/37. Considering the span of the superstructure, it is obvious, that the full width of the concrete slab interact with the steel girder. Effective equivalent steel cross-section parameters are determined for the further calculation. Since the calculation of reaction moduli comprehends long-term and short-term actions, the elasticity modulus of the concrete is set approximately:

$E_c' = E_{cm} / 2 = 32\,000 / 2 = 16\,000$ MPa

Modular ratio is calculated as follows:

$$n = E_a / E'_c = 210\,000 / 16\,000 = 13{,}1$$

All needed equivalent cross-section characteristics of the superstructure have to be determined. Elimination of the reinforced concrete slab in the areas of hogging moments near to the abutments can be neglected for the calculation of the reaction moduli. Reinforcement of the concrete slab is neglected too. Thus, we consider the full steel-concrete cross-section neglecting the reinforcement of the slab along the whole length of the superstructure. The equivalent cross-section characteristics in segments 1, 2 and 3 of the superstructure are:

Segments 1 and 3 $A_{eff} = 0{,}116\ m^2$ $I_{eff,y} = 57{,}014 \cdot 10^{-3}\ m^4$

Segment 2 $A_{eff} = 0{,}106\ m^2$ $I_{eff,y} = 41{,}282 \cdot 10^{-3}\ m^4$

Abutment and Footing

Cross-sections of the abutment and of the footing are shown in Figures 5.6b and 5.6c. The material of the both cross-sections is concrete C25/30 with the modulus of elasticity $E_{cm} = 30\,500$ MPa.

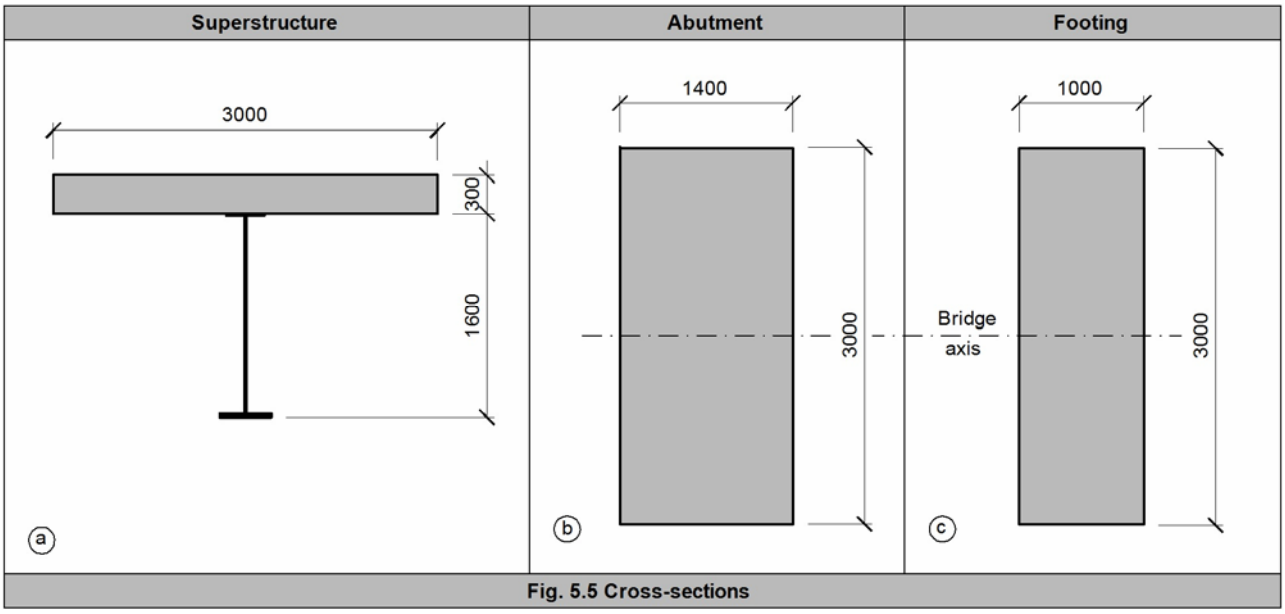

Fig. 5.5 Cross-sections

Distributed Linear Springs on the Abutments and Footings

The stiffness of the distributed linear springs placed on the abutments and on the spread footings can be generally calculated from the moduli of subgrade reaction. As mentioned in Chapter 2, moduli of subgrade reaction represent physically the stiffness of the surface spring supporting surface elements. However, in case of the planar model, the distributed linear springs supporting the members of the abutments and the footings are used. The stiffness of the distributed linear springs (kN/m^2) can be calculated by multiplying the moduli of subgrade reaction (kN/m^3) by the considered width, in our case, by the width of 3 m.

The linear spring on the abutments acts in the horizontal direction, i.e. perpendicular to the abutment, when the abutment is pushed into the backfill. Since the k_h value is variable, see chapter 3, the stiffness K_h of the linear spring is variable too. The stiffness K_h of the linear spring is in each point of the abutment equal to:

$$K_h = k_h \cdot 3{,}0$$

The linear spring placed to the footing members acts in two perpendicular directions:

- In the vertical direction, i.e. perpendicular to the footing. Vertical stiffness K_z is calculated:
  $K_z = k_z \cdot 3{,}0$
- In the horizontal direction, i.e. parallel with the footing. Horizontal stiffness K_x is calculated:
  $K_x = k_x \cdot 3{,}0$

To calculate the values of the stiffness K_h, K_z and K_x, it is necessary to have the values of reaction moduli k_h, k_z and k_x. These values are unknown at the moment, because they are the aim of this calculation. Therefore, in the first step of the calculation, the distributed linear springs supporting the spread footings are substituted by rigid nodal supports and the springs on the abutments are ignored. The structural model for the first step of the calculation is shown in Figure 5.12.

2. Actions

In the calculation of the reaction moduli k_h, k_z and k_x, we will consider the actions, which significantly contribute to the horizontal and vertical stress in the footing bottom and to the horizontal displacements of the abutment towards to the backfill. These include:

- Self-weight (G),
- Uniformly distributed load due to traffic (UDL), according to [5],
- Tandem system traffic load (TS) according to [5],
- Temperature load (TEM), according to [4].

Self-Weight Load (G)

Self-weight load includes the self-weight of the footings, the abutments and the superstructure including other non-bearing elements. The load is applied to the 3,0 m wide longitudinal cut-out of the bridge including one main girder. The self-weight load is determined as a continuous uniformly distributed load; see the following tables:

Superstructure and other non-bearing elements in 3 m wide strip

Reinforced concrete slab		0,3 . 25 . 3,0 =	22,5 kN/m
Steel girder:	segments 1 and 3	0,0475 . 78,5 =	3,7 kN/m
	segment 2	0,0379 . 78,5 =	3,0 kN/m
Pavement and insulation		0,09 . 25 . 3,0 =	6,8 kN/m
Total:	segments 1 and 3		**33,0 kN/m**
	segment 2		**32,3 kN/m**

Abutments in 3 m wide strip

Abutment body	1,4 . 25 . 3,0 =	**105,0 kN/m**

Footing in 3 m wide strip 3 m

Foundation	1,0 . 25 . 3,0 =	**75,0 kN/m**

The resulting diagram of the self-weight load is shown in Figure 5.6.

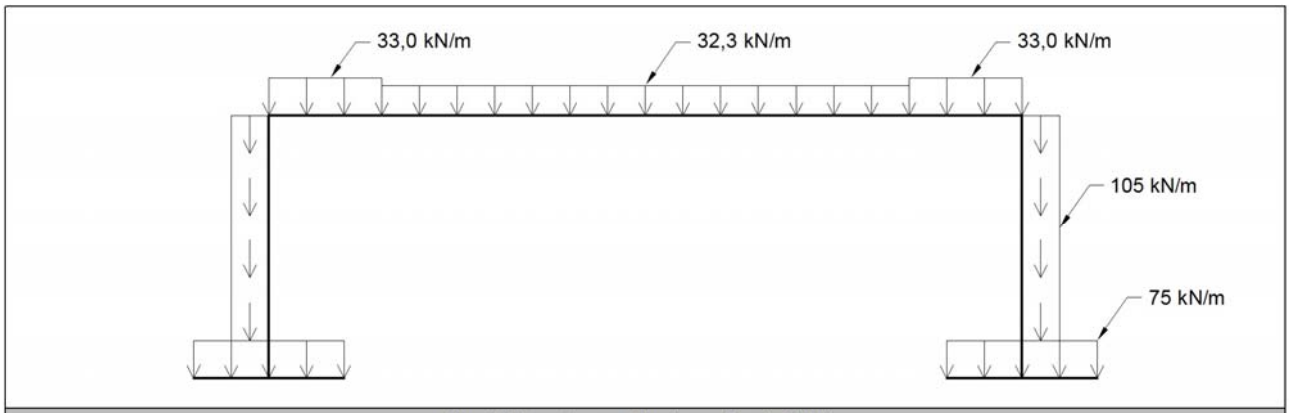

Fig. 5.6 Load case due to self-weight (G)

Uniformly Distributed Traffic Load (UDL)

Uniform load distribution on the area of the bridge according to [5] is shown in Figure 5.7. Adjustment factors for the road group 1 are considered by values $\alpha_{q1} = 0,8$ and $\alpha_{q2} = 1,0$.

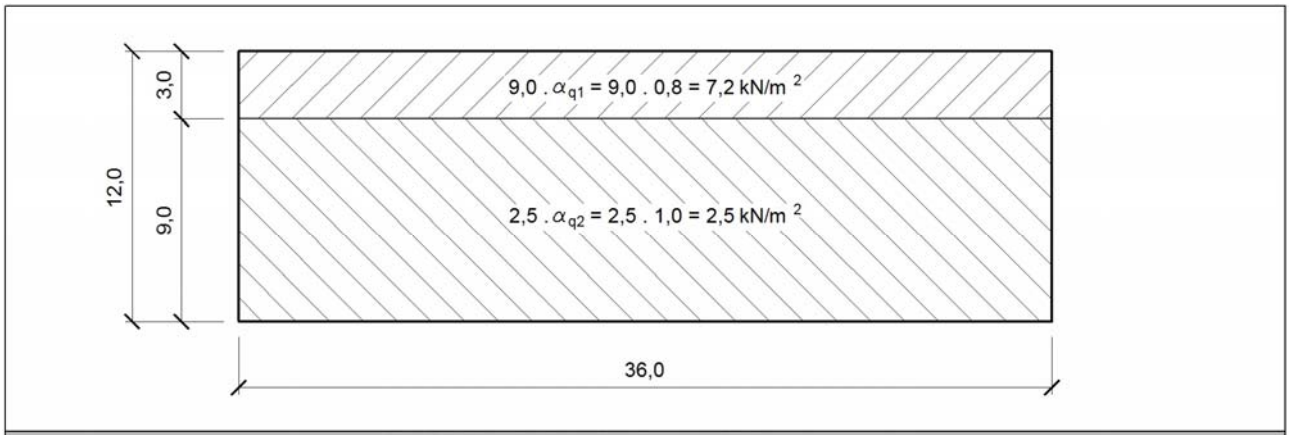

Fig. 5.7 Distribution of uniform traffic load on bridge

For purposes of the calculation of stress in the footing bottom, it is possible to average the load on the bridge area and transform it to the linear load f_{UDL} of 3 m wide strip.

$$f_{UDL} = \left(\frac{7,2 \,.\, 3,0 + 2,5 \,.\, 9,0}{12,0} \right) \,.\, 3,0 = 11,025 \text{ kN/m}$$

The resulting diagram of the uniformly distributed load is shown in Figure 5.8.

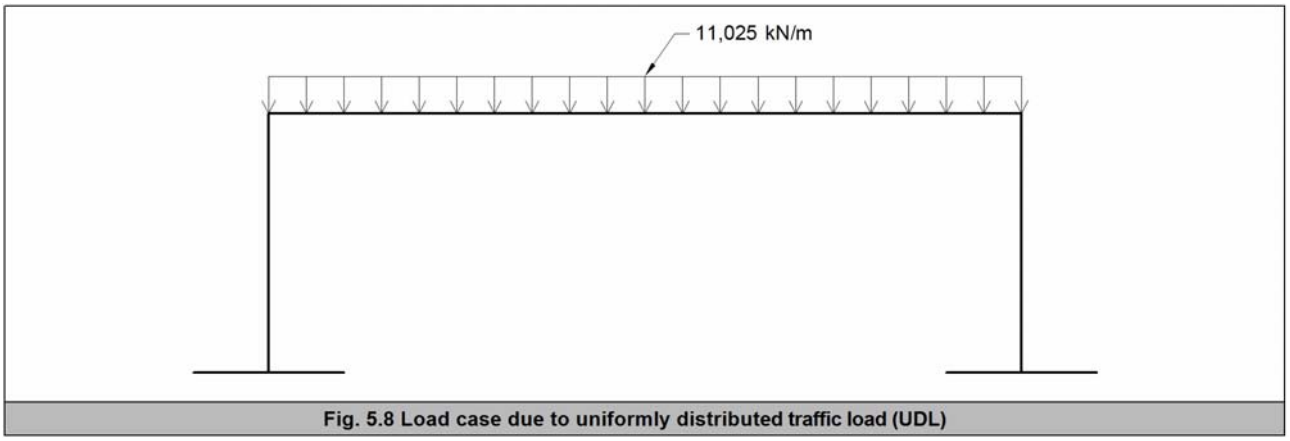

Fig. 5.8 Load case due to uniformly distributed traffic load (UDL)

Tandem System Load (TS)

Distribution of the tandem axle on the bridge area according to [5] is shown in Figure 5.9. Considering, we calculate the 'global' stiffness of the soil springs, which are constant for all positions of the live load, the tandem axle is placed to give the maximum effect on the superstructure, i.e. to the middle of the span. Adjustment factors for the road group 1 are considered by values $\alpha_{Q1} = \alpha_{Q2} = \alpha_{Q3} = 0,8$.

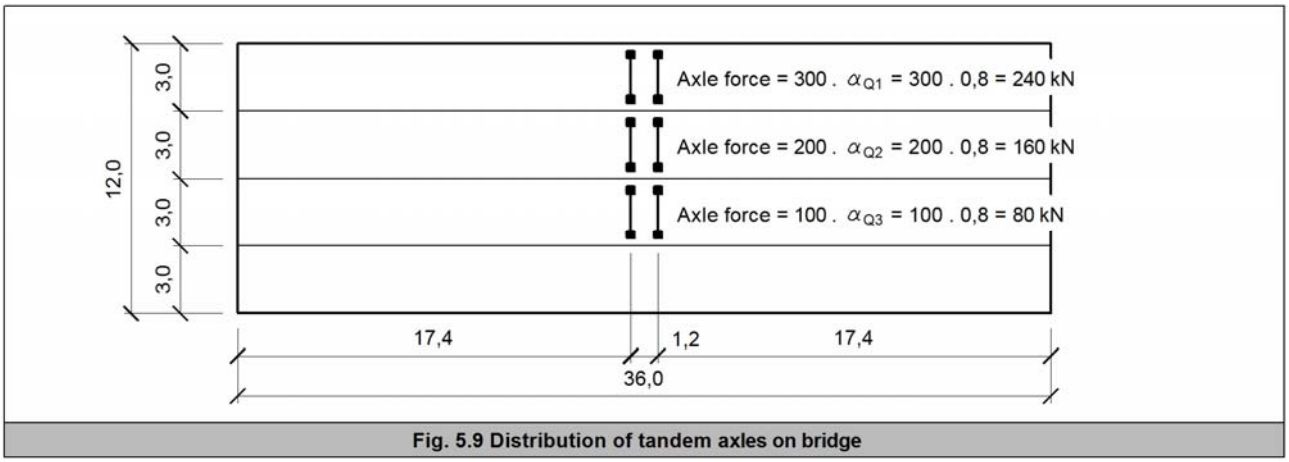

Fig. 5.9 Distribution of tandem axles on bridge

For purposes of calculation of stresses in the footing bottom, it is possible to average the tandem system load and transform it to the concentrated loads F_{TS} in 3 m wide strip.

$$F_{TS} = \left(\frac{240 + 160 + 80}{12,0} \right) . 3,0 = 120 \text{ kN}$$

The resulting diagram of the tandem system load is shown in Figure 5.10.

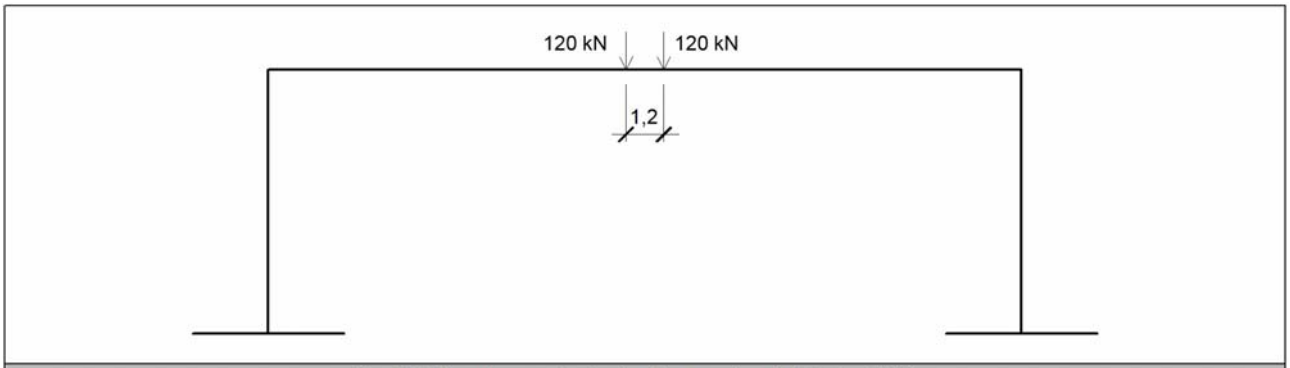

Fig. 5.10 Load case due to tandem system traffic load (TS)

Temperature Load (TEM)

The uniform temperature component $\Delta T_{N, exp}$ for calculation of the bridge extension is determined according to [4]. The maximum shade air temperature is set to T_{max} = 40ºC. For the composite steel-concrete bridges, the maximum uniform temperature component of the bridge is set to $T_{e, max}$ = 45ºC. The initial temperature of the bridge at time of installation is set to T_0 = 10ºC.

The uniform temperature component $\Delta T_{N, exp}$ for calculation of the bridge extension is determined as follows:

$$\Delta T_{N, exp} = T_{e, max} - T_0 = 45 - 10 = 35 \text{ ºC}$$

The resulting diagram of the temperature load is shown in Figure 5.11.

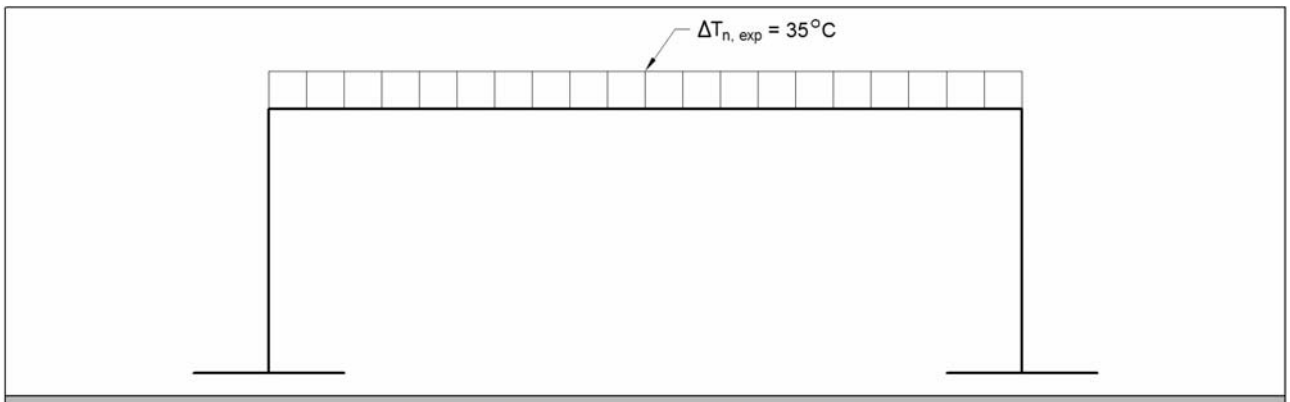

Fig. 5.11 Load case due to thermal action (TEM)

Combinations of Actions

In this example, the calculation of the moduli of subgrade reaction is based on the frequent combination[5.3] according to [3]. In our case, this combination takes a form:

$G_k + \psi_1 . Q_{k1} + \psi_2 . Q_{k2}$

where: G_k is permanent action,
Q_{k1} leading variable action,
Q_{k2} accompanying variable loads,
ψ_1, ψ_2 combination factors.

Using load cases defined above, two frequent combinations are created:

1) **Combination 1** is used to calculate reaction moduli k_h. The variable thermal action is considered as leading with combination factor $\psi_1 = 0,6$. The traffic action is considered as accompanying with combination factor $\psi_2 = 0,0$. The deformations due to permanent action occur mainly before the backfill exists. Therefore, the permanent action is not included in combination 1. Combination 1 is assumed as:
   Combination 1 = 0,6 TEM

2) **Combination 2** is used to calculate reaction moduli k_z and k_x. The variable traffic action is considered as leading with combination factor $\psi_1 = 0,75$ for TS and $\psi_1 = 0,4$ for UDL. The thermal action is considered as accompanying with combination factor $\psi_2 = 0,5$. Combination 2 is then assumed as:
   Combination 2 = G + 0,75 TS + 0,4 UDL + 0,5 TEM

Note 5.3: This example demonstrates a simple way of the practical process of calculation of the moduli of subgrade reaction k_h, k_z and k_x and of the stiffness of the soil springs K_h, K_z and K_x supporting the integral bridge. Therefore, only one 'representative' load combination for calculation of stiffness K_h and only one load combination for calculation of stiffness K_z and K_x is used. The distributed springs modeling the elastic support of the bridge are linear, see Note 2.1. The frequent load combination was chosen for calculation of the spring stiffness, because it represents the 'frequent' actions on the bridge. In addition, the frequent load combination is normally used to verify the bearing capacity of subsoil. In the example, the stiffness K_h, K_z and K_x calculated from the frequent load combination are used universally for all other load combinations used for the bridge design. However, this simplified approach is not a common rule. For calculation of the stiffness K_h, K_z and K_x, it is also possible to use different load combinations according to the actual case and consideration of the project engineer. In case of insufficient fidelity of usage of one representative values of K_h, K_z and K_x, it is possible to calculate two boundary stiffnesses of K_h, K_z and K_x: rigid and soft. Afterwards, two structural models are created: one with 'rigid' values of K_h, K_z and K_x and the other with 'soft' values of K_h, K_z and K_x. The envelope of results of both structural models is then used for the bridge design. This procedure is often used in practice. It takes into the account the real non-linear soil behavior and compensates the common uncertainty in calculation of the moduli of subgrade reaction.

3. Calculation of Stiffness K_h, K_z and K_x of Soil Springs

Since the stiffness K_h, K_z and K_x of the soil springs depends on the horizontal displacements of the abutments, respectively on the stress in the footing bottom, the calculation is carried out in several steps. Stiffness K_h, K_z and K_x calculated in the previous step are used as an input for the next step.

1st Step of Calculation

Since the horizontal displacements of the abutment required for calculation of K_h are unknown at this moment, the soil springs on the abutments are not included to the structural model in the first step of the calculation. Considering, the stress in the footing bottom, required to calculate K_z and K_x, is unknown as well, the horizontal and vertical support of the abutments is regarded as pined nodal supports. The structural model for the first step of the calculation is shown in Figure 5.12.

Fig. 5.12 Structural model for the first step of calculation

Analysis results required for calculation of the reaction moduli k_h, k_z and k_x are shown in Figure 5.13.

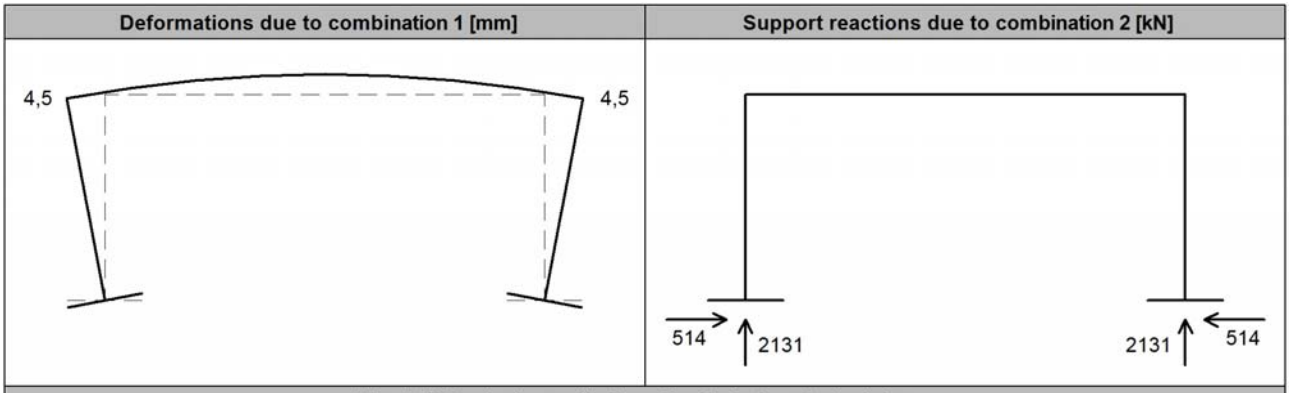

Fig. 5.13 Analysis results from the first step of calculation

Now, the reaction moduli k_h and resulting soil spring stiffness K_h can be determined. Analysis results show that the horizontal displacement at the top of the abutment u_T = 4,5 mm and the horizontal displacement at the bottom of the abutment u_B = 0,0 mm. Thus, rotation of the abutment is regarded. The distribution of the reaction moduli k_h corresponds to bilinear curve R. To determine curve R, see Figure 3.1, it is necessary to calculate values $k_{h,\,1}$, $k_{h,\,2R}$, $k_{h,\,3R}$ and z_2 according to formulas in Table 3.1. Factors A, B, C and D can be found in Table B.1, Annex B. Since the height of the abutment H_a is equal to 9,5 m in the structural model, we need to interpolate between the values of heights 9 and 10 m in Table B.1.

$$k_{h,1} = \frac{A_1\, E_{ref}\, u_T}{10^4} + \frac{B_1\, E_{ref}}{10^2} + \frac{C_1\, u_T}{10^2} + D_1 = \frac{-3{,}3 \,.\, 40 \,.\, 4{,}5}{10^4} + \frac{3{,}5 \,.\, 40}{10^2} + \frac{0{,}0 \,.\, 4{,}5}{10^2} + 0{,}0 = 1{,}3 \text{ MN/m}^3$$

$$k_{h,2R} = \frac{A_2\, E_{ref}\, u_T}{10^4} + \frac{B_2\, E_{ref}}{10^2} + \frac{C_2\, u_T}{10^2} + D_2 = \frac{-0{,}85 \,.\, 40 \,.\, 4{,}5}{10^4} + \frac{11{,}25 \,.\, 40}{10^2} + \frac{0{,}0 \,.\, 4{,}5}{10^2} + 0{,}55 = 5{,}0 \text{ MN/m}^3$$

$$k_{h,3R} = k_{h,2R} = 5{,}0 \text{ MN/m}^3$$

$$z_2 = \frac{A_z\, E_{ref}\, u_T}{10^4} + \frac{B_z\, E_{ref}}{10^2} + \frac{C_z\, u_T}{10^2} + D_z = \frac{1{,}85 \,.\, 40 \,.\, 4{,}5}{10^4} + \frac{0{,}15 \,.\, 40}{10^2} + \frac{1{,}0 \,.\, 4{,}5}{10^2} + 0{,}95 = 1{,}1 \text{ m}$$

Stiffnesses of the distributed soil springs on the abutments are then calculated as follows:

$K_{h,1} = k_{h,1} \,.\, 3{,}0 = 1{,}3 \,.\, 3{,}0 =$ **3,9 MN/m²**

$K_{h,2R} = k_{h,2R} \,.\, 3{,}0 = 5{,}0 \,.\, 3{,}0 =$ **15,0 MN/m²**

$K_{h,3R} = k_{h,3R} \,.\, 3{,}0 = 5{,}0 \,.\, 3{,}0 =$ **15,0 MN/m²**

The final distribution of the reaction moduli k_h and the spring stiffness K_h on the abutment is shown in Figure 5.14.

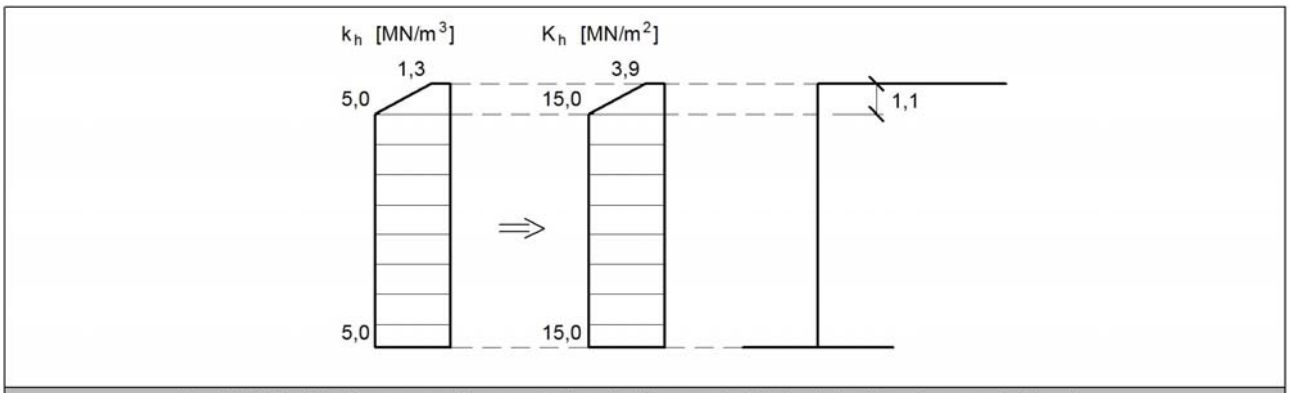

Fig. 5.14 Distribution of reaction moduli and stiffness of distributed soil springs on abutment

Now, reaction moduli k_z and k_x are calculated using formulas (4.1) and (4.2). Homogenous subsoil below the footing consisting of sandy soil classified as SF is assumed. Factors K, L, M, N are obtained from Table C.1, Annex C. We need to interpolate in table according to the length and the width of the footing. In case of footing dimensions 5x12 m, the final interpolated factors are:

K = 1204,0 L = 36,0 M = 1,66 N = 21,0

According to the analysis results from combination 2, vertical stress in the footing bottom is:

$$f_z = \frac{2131}{3{,}0 \,.\, 5{,}0} = 142 \text{ kN/m}^2$$

Depth of the compressible subsoil H_s is obtained by interpolation in Table F.1, Annex F. Subsoil consisting of soil classified as SF is assumed. In case of footing dimensions 5x12 m and vertical stress in the footing bottom f_z = 142 kN/m² the final interpolated value of H_s is:

H_s = 6,1 m

The layer of the SF soil is 9,0 m depth. Thus, entire compressible subsoil, where significant deformations of subsoil occur, consists of SF soil only. The groundwater level is 7,0 m below the footing bottom. Therefore, it is outside of the compressible subsoil. In this case, influence of groundwater can be neglected. W_z is obtained from Table E.1, Annex E:

$W_z = 1,0$

Using formula (4.1), we get:

$$k_z = \left(\frac{K}{L + f_z} + M \right) \frac{E_{ref}}{N} W_z = \left(\frac{1204,0}{36,0 + 142} + 1,66 \right) \frac{21,0}{21,0} \; 0,95 = 8,0 \text{ MN/m}^3$$

Factors P, Q, R, S, T, U are obtained by interpolation in Table D.1, Annex D. In case of footing dimensions 5x12 m, the final interpolated factors are:

P = 0,0055 Q = 2,9 R = 50,0 S = 0,0082 T = 6,7 U = 8,1

Factor W_x can be determined from Table E.1, Annex E. As already mentioned, the groundwater level is outside of the compressible zone. From Table E.1 follows:

$W_x = 1,0$

According to the analysis results from combination 2, horizontal stress in the footing bottom is:

$$f_x = \frac{514}{3,0 \,.\, 5,0} = 34 \text{ kN/m}^2$$

Using formula (4.2), we get:

$$k_x = \left(\frac{P \, f_x \, f_z - Q \, f_x}{R} - S \, f_z + T \right) \frac{G_{ref}}{U} W_x = \left(\frac{0,0055 \,.\, 34 \,.\, 142 - 2,9 \,.\, 34}{50,0} - 0,0082 \,.\, 142 + 6,7 \right) \frac{8,0}{8,1} 1,0 =$$

$$= 4,0 \text{ MN/m}^3$$

Stiffnesses of the distributed soil springs on the footing are then calculated as follows:

$K_z = k_z \,.\, 3,0 = 8,4 \,.\, 3,0 =$ **25,2 MN/m²**

$K_x = k_x \,.\, 3,0 = 4,0 \,.\, 3,0 =$ **12,0 MN/m²**

2nd Step of Calculation

The structural model for the second step of the calculation is shown in Figure the 5.15. The stiffness of distributed soil springs were calculated in the first step of calculation.

Fig. 5.15 Structural model for the second step of calculation

Analysis results are shown in Figure 5.16. Using these results, reaction moduli k_h, k_z and k_x are calculated.

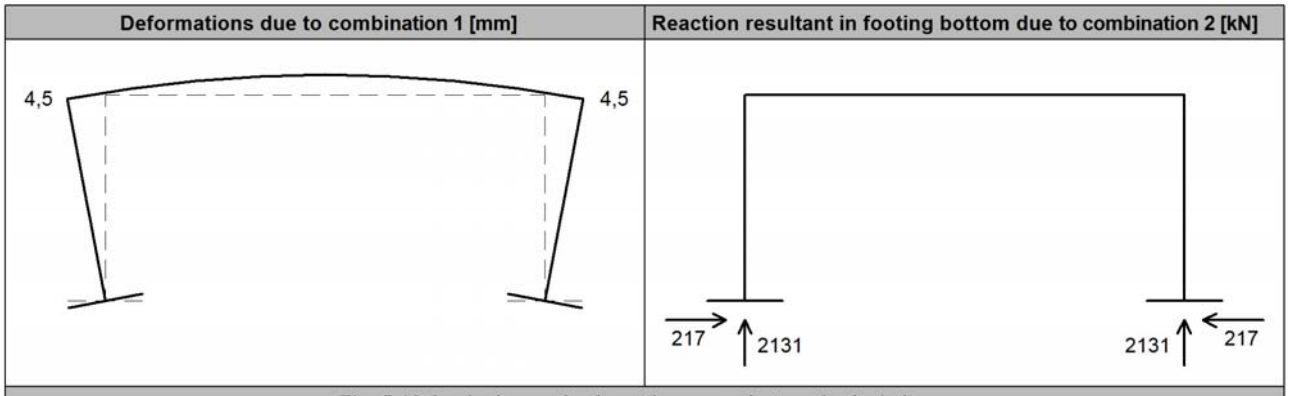

Fig. 5.16 Analysis results from the second step of calculation

The analysis results show, that u_T = 4,5 mm and u_B = 0,0 mm. These values do not differ from the first step. Thus, we consider the reaction moduli k_h and the stiffness of soil springs K_h equal to the values in the first step. The reaction modulus k_z also remains the same. Calculation of the reaction modulus k_x is analogous to the first step. Factors P, Q, R, S, T, U and W_x remain unchanged.

$$f_x = \frac{217}{3{,}0\,.\,5{,}0} = 14{,}5\ \text{kN/m}^2$$

$$k_x = \left(\frac{P\,f_x\,f_z - Q\,f_x}{R} - S\,f_z + T \right) \frac{G_{ref}}{U}\,W_x = \left(\frac{0{,}0055\,.\,14{,}5\,.\,142 - 2{,}9\,.\,14{,}5}{50{,}0} - 0{,}0082\,.\,142 + 6{,}7 \right) \frac{8{,}0}{8{,}1}\,1{,}0 =$$

$$= 4{,}9\ \text{MN/m}^3$$

As well as in the first step of the calculation, the entire compressible subsoil consists of SF soil only. Consequently, the linear spring stiffnesses placed on the footing can be determined as follows:

$K_z = k_z\,.\,3{,}0 = 8{,}4\,.\,3{,}0 =$ **25,2 MN/m²**

$K_x = k_x\,.\,3{,}0 = 4{,}9\,.\,3{,}0 =$ **14,7 MN/m²**

3rd Step of the Calculation

The structural model for the third step of the calculation is shown in Figure 5.17. The stiffness of distributed soil springs were calculated in the second step of the calculation.

Fig. 5.17 Structural model for the third step of calculation

Analysis results are shown in Figure 5.18. Using these results, reaction moduli k_h, k_z and k_x are calculated.

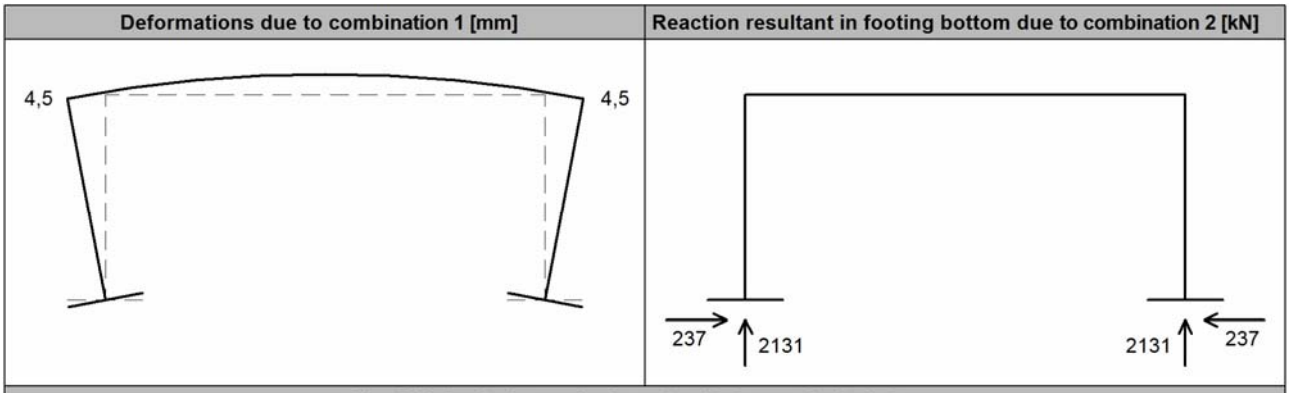

Fig. 5.18 Analysis results from the third step of calculation

The horizontal displacements of the abutment imply that the distribution of the reaction moduli k_h remains unchanged in the third step as well. In addition, the reaction modulus k_z remains the same. Calculation of the reaction modulus k_x is analogous to the first and the second step. Factors P, Q, R, S, T, U and W_x remain the same as well.

$$f_x = \frac{237}{3{,}0\,.\,5{,}0} = 15{,}8\ \text{kN/m}^2$$

$$k_x = \left(\frac{P\,f_x\,f_z - Q\,f_x}{R} - S\,f_z + T \right) \frac{G_{ref}}{U}\,W_x = \left(\frac{0{,}0055\,.\,15{,}8\,.\,142 - 2{,}9\,.\,15{,}8}{50{,}0} - 0{,}0082\,.\,142 + 6{,}7 \right) \frac{8{,}0}{8{,}1}\,1{,}0 =$$

$$= 4{,}8\ \text{MN/m}^3$$

When comparing the reaction moduli k_h, k_z and k_x from the second and the third step of the calculation, we conclude that they are practically identical. The reaction moduli from the third step of the calculation can be considered as final and the calculation can be terminated.

4. Conclusion

The final values and distributions of the moduli of subgrade reaction k_h, k_z and k_x are summarized in Figure 5.19. These values can be used as parameters of elastic subsoil for the design of integral bridge. We suppose that above calculated reaction moduli are used 'universally' for any positions of the traffic load.

Fig. 5.19 Final reaction moduli

If we use the same planar structural model for further design (Example 4), i.e. 3 m wide longitudinal cut-out of the bridge structure, the stiffness of distributed linear springs supporting the substructure are summarized in Figure 5.20.

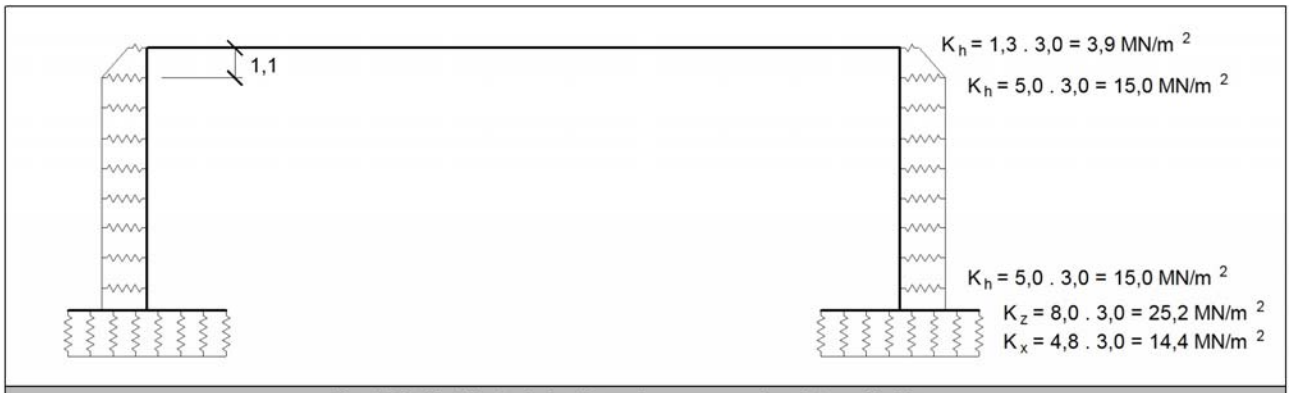

Fig. 5.20 Distributed elastic springs supporting integral bridge

5.4 Example 4

Check the superstructure of the integral bridge from example 3 in the ultimate limit state.

---

1. Assumptions

The check is based on following assumptions and simplifications [5.4]:

1) Construction without falsework is expected. Construction stages are considered in the check, see paragraph 2.
2) In the check, elastic stress distribution in the cross section is expected. Shear lag of flanges and buckling of web is neglected. Full cross-section characteristics are used.
3) The influence of shrinkage and creep of concrete is neglected. Non-uniform change of temperature and settlement of supports is not considered.

2. Structural Model and Construction Stages

Simplified planar structural model from example 3 is used. The planar model represents 3 m wide longitudinal cut-out of the bridge structure comprehending one main girder. The width of the cut-out corresponds to the spacing of steel girders. The structural model includes the superstructure and the substructure, because of the mutual interaction. Cross-section of the superstructure, the abutment and the footing are shown in Figure 5.5, see example 3. The structural model varies depending on the construction stage, whereas different load cases act in each stage. Depending on the construction stage, adjacent soil is represented by load or by distributed springs placed on the substructure elements. The stiffness of springs is calculated in example 3. Construction sequence is divided into four stages; see Figure 5.21:

1) In the first construction stage, the steel girders are mounted on the abutments. The connection of the superstructure to the abutments is hinged. Elastic supports are placed on the footings only, because the backfill behind the abutments does not exist yet. The structure is loaded by self-weight of the steel girder (G_a). The self-weight of the substructure is neglected, because it has no effect to the superstructure. The effective cross-section of the superstructure consists of the steel girder only.

2) In the second construction stage, the capping beams are concreted, whereby the superstructure is fixed to the substructure. Then the reinforced concrete slab is concreted. The structure is loaded by the self-weight of the slab (G_c). The effective cross-section of the superstructure remains the steel girder only.

3) In the third construction stage, after hardening of the reinforced concrete slab, backfills behind the abutments are made. Backfilling and compaction of the backfill is carried out in layers in turns by the first and the second support to prevent from significant asymmetric horizontal loads due to horizontal soil pressures. The abutments are loaded by earth pressure at rest (S_0). In the middle part of the superstructure (segment 2), where sagging bending moments are expected, the superstructure performs as a full composite girder.

Note 5.4: These assumptions are simplifications used in this actual example only to make the calculation brief and clear. These are not the general rules, which are commonly followed by the design and check of integral bridges.

In the marginal segments by abutments (segment 1 and 3), the effective cross-section of the superstructure consist of the steel girder and the reinforcement in the slab. The length of segments 1 and 3, where cracks in the concrete slab due to hogging bending moments occurs, is expected to be equal to the 6 m, universally for all load cases. This length is estimated as 1/6 of the superstructure span.

4) In the fourth construction stage, the pavement and other bridge equipment is finished. The distributed linear soil springs simulating the effect of the backfill are added into the structural model. The structure is loaded by the permanent load due to pavement and bridge equipment (G_{fin}), by uniformly distributed traffic load (UDL), by tandem system load inducing maximal effects in the particular sections of the superstructure (from TS_1 to TS_{30}) and by the uniform temperature load (TEM). The effective cross-sections of the superstructure are the same as in the third stage.

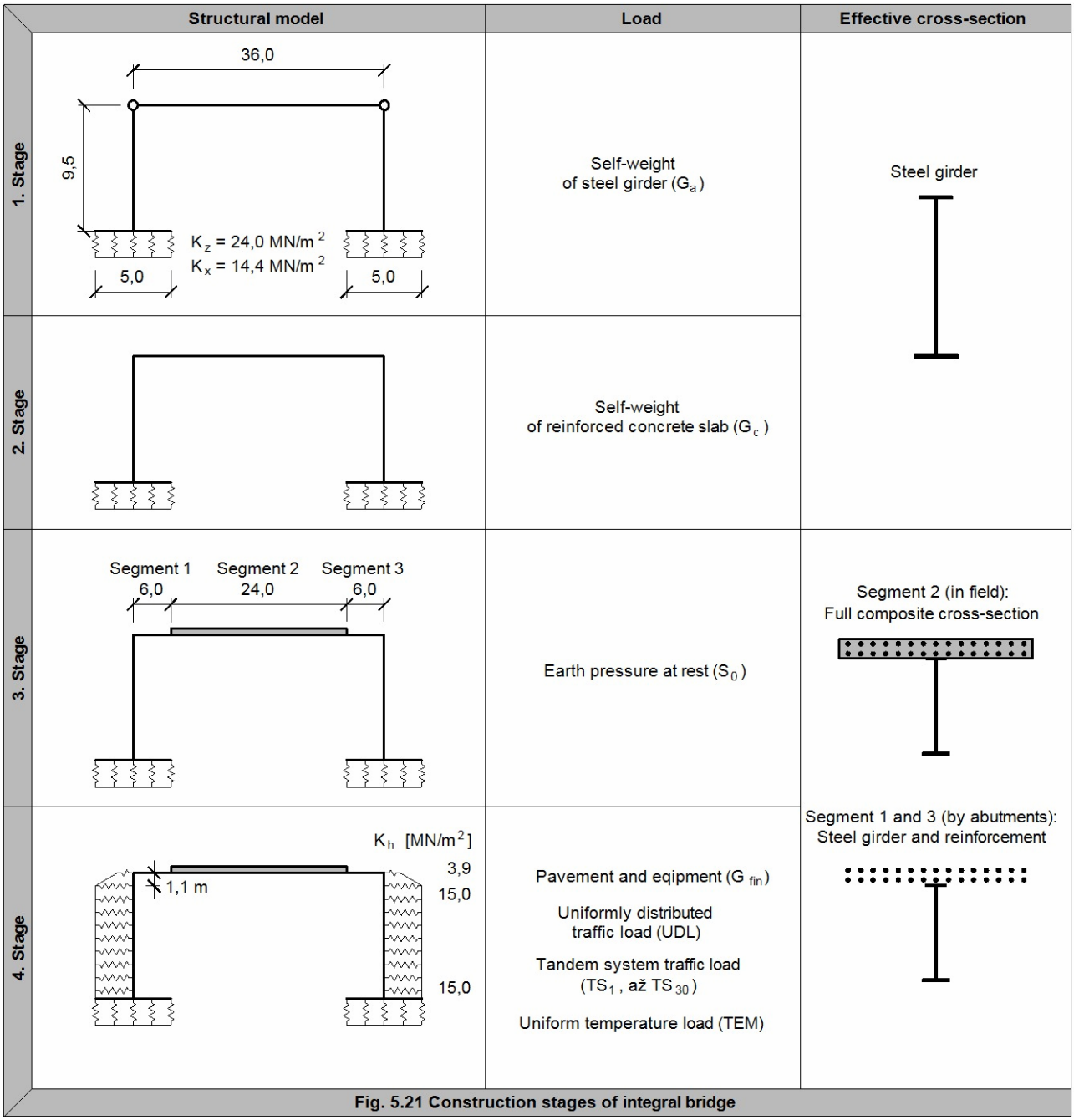

Fig. 5.21 Construction stages of integral bridge

3. Actions

The load cases shown in Figure 5.21 are specified in this paragraph. The diagrams of the particular load cases are summarized in Figure 5.22.

Self-Weight, Temperature Load and Uniformly Distributed Load due to Traffic (G_a, G_c, TEM, UDL)

The values of the loads for load cases G_a, G_c, TEM, UDL are taken from example 3.

Pavement and Bridge Equipment Load (G_{fin})

In load case G_{fin}, loads due to pavement and insulation are considered only. The value of the load is taken from example 3.

At Rest Earth Pressure Load (S_0)

For backfill soil SP, bulk density is considered $\gamma = 18{,}5$ kN/m^3 and friction angle $\varphi = 35{,}5°$. Earth pressure at rest is considered as continuous triangular load acting on the abutments in the horizontal direction. The load is related to the 3,0 m wide longitudinal cut-out of the bridge. Its value at the top of the abutment is zero, value at the bottom is as follows:

$$f_{S0} = (1 - \sin\varphi) \cdot H_a \cdot \gamma \cdot 3{,}0 = (1 - \sin 33{,}5) \cdot 9{,}5 \cdot 18{,}5 \cdot 3{,}0 = 236{,}2 \text{ kN/m}$$

Diagram of load case S_0 is shown in Figure 5.22.

Tandem System Traffic Load (TS_1 to TS_{30})

In the load cases TS_1 to TS_{30}, tandem system is placed to induce maximal bending moments in particular cross-sections of the superstructure. In the load case TS_1, tandem system is placed next to the left abutment. In the following load cases from TS_2 to TS_{30}, the tandem system is always shifted 1,2 m towards to the right abutment. The values of the tandem system forces are taken from example 3. Diagrams of load cases TS_1, TS_2 and TS_{30} are shown in Figure 5.22.

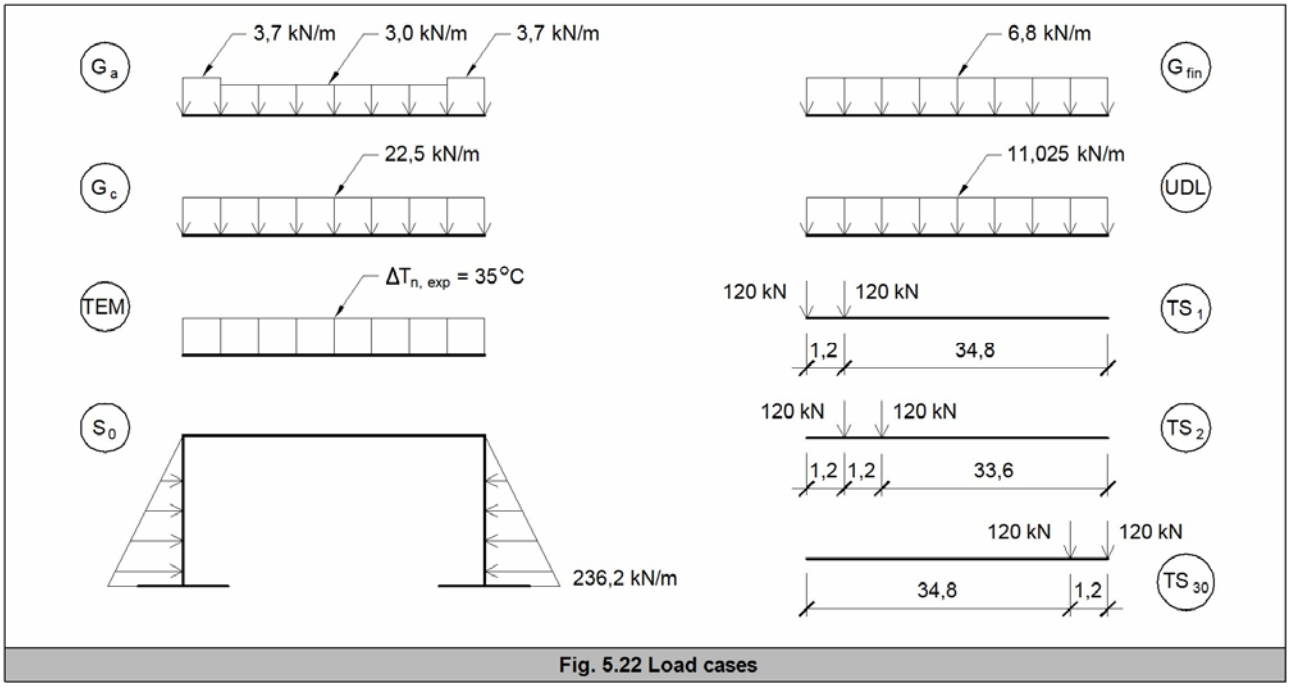

Fig. 5.22 Load cases

Combination of Actions for the Ultimate Limit State Check

To carry out the ultimate limit state check, load combination according to [3] is created, where the traffic load is considered as leading. The combination is as follows:

$$ULS = 1{,}35 \cdot (G_a + G_c + S_0 + G_{fin}) + 1{,}5 \cdot (UDL + TS_{env}) + 1{,}5 \cdot 0.6 \cdot TEM$$

where: TS_{env} is an envelope of the load cases TS_1 to TS_{30}.

4. Analysis Results

Linear analysis was carried out for each load case. The results for ULS combination were obtained by linear superposition of load cases G_a, G_c, S_0, G_{fin}, UDL, TEM and the envelope TS_{env}. Figures 5.23, 5.24 and 5.25 show normal stress distributions along the superstructure due to ULS combination. Normal stress in the steel girder, in reinforcement of the deck, and in concrete of the deck are displayed. Since TS_{env} envelope is included in the combination, the normal stress distributions are bifurcated to maximal and minimal branches.

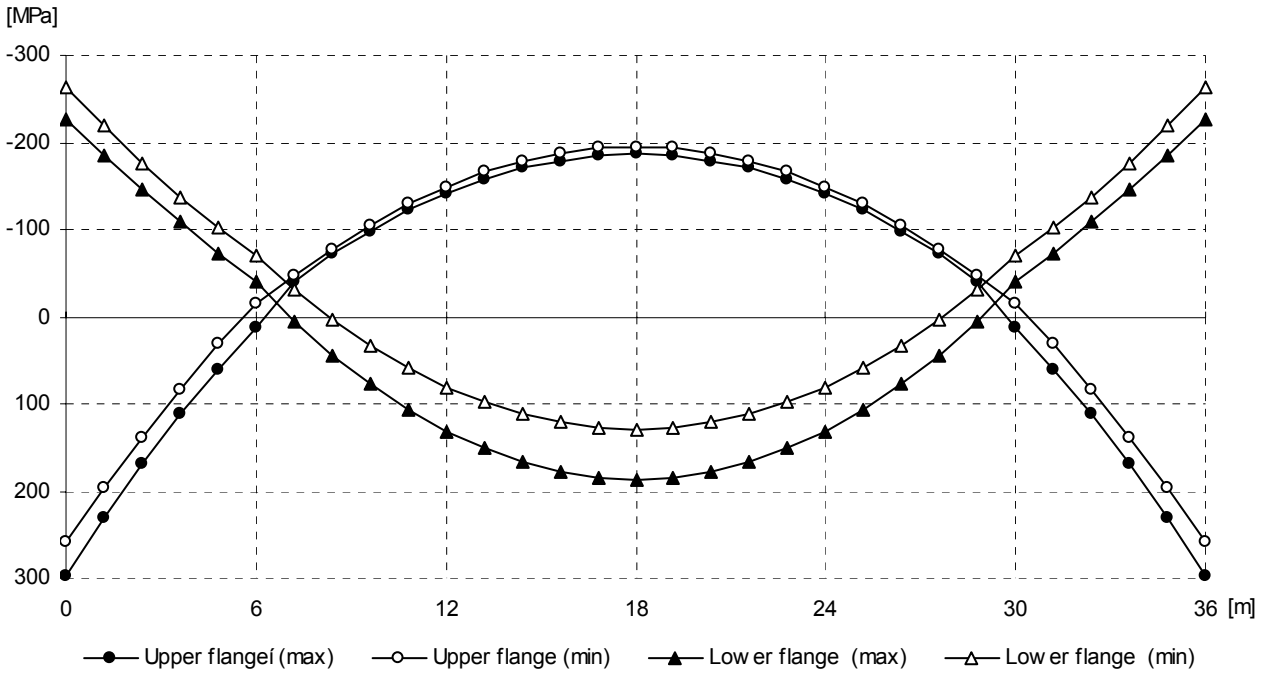

Fig. 5.23 Distribution of normal stress in upper and lower flange of steel girder

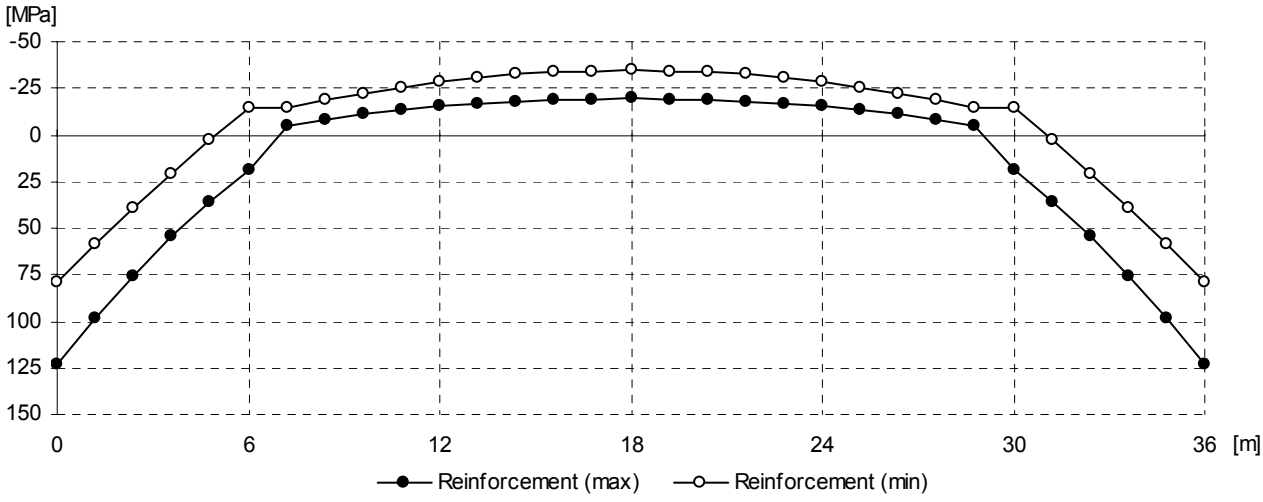

Fig. 5.24 Distribution of normal stress in reinforcement of slab

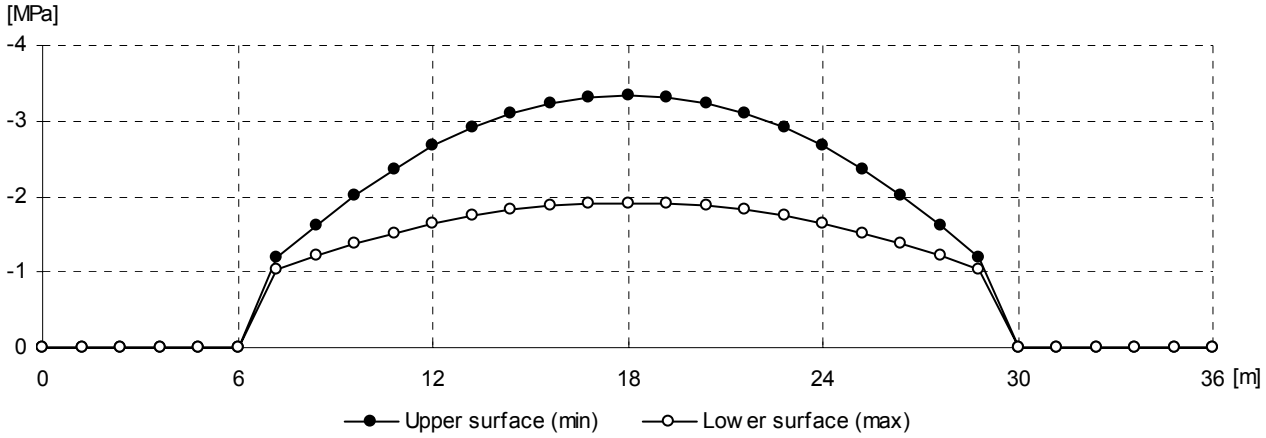

Fig. 5.25 Distribution of normal stress in concrete of slab

Upon the calculated results, check of the steel girder, the reinforcement and the concrete can be done:

- Steel girder: $f_{yd} = 335 / 1{,}0 = 335{,}0$ MPa > $\sigma_{max} = 296{,}9$ MPa => OK
- Reinforcement: $f_{yd} = 490 / 1{,}0 = 490{,}0$ MPa > $\sigma_{max} = 124{,}0$ MPa => OK
- Concrete: $f_{cd} = 0{,}85 \cdot 30 / 1{,}5 = 17{,}0$ MPa > $\sigma_{max} = 3{,}3$ MPa => OK

5. Conclusion

The calculation proved, the superstructure of the integral bridge satisfies in the ULS check. It should be noted, the calculation was based on the simplified assumptions mentioned in paragraph 1 at the beginning of this example. When more detailed check is carried out, it is necessary to include the effects of shrinkage and creep of the reinforced slab, buckling of the web and shear lag of the flanges of the steel girder. It is also necessary to consider loads due to support settlement and due to the non-uniform temperature change. In addition to the ultimate limit state, it is necessary to check the serviceability limit state. SLS check of crack width of the concrete slab in the area of hogging bending moments is very important and often decisive criterion.

ANNEX A – SOIL PARAMETERS

Table A.1 Sandy soils							
Class	Symbol	γ [kN/m^3]	ν [-]	φ [°]	c [kPa]	E_{ref} [MPa]	G_{ref} [MPa]
S1	SW	20,0	0,28	37 - 42	0	50 - 100	19 - 39
S2	SP	18,5	0,28	34 - 37	0	30 - 50	12 - 20
S3	SF	17,5	0,30	30 - 33	0	17 - 25	6 - 10
S4	SM	18,0	0,30	28 - 30	0 - 10	5 - 15	2 - 6
S5	SC	18,5	0,35	26 - 28	4 - 12	4 - 12	1,5 - 4,5
Soil parameters in Table A.1 correspond to the index of relative density I_D > 0,67							

Table A.2 Gravelly soils							
Class	Symbol	γ [kN/m^3]	ν [-]	φ [°]	c [kPa]	E_{ref} [MPa]	G_{ref} [MPa]
G1	GW	21,0	0,20	39 - 44	0	360 - 500	150 - 210
G2	GP	20,0	0,20	36 - 41	0	170 - 250	70 - 104
G3	GF	19,0	0,25	33 - 38	0	90 - 100	36 - 40
G4	GM	19,0	0,30	30 - 35	0 - 8	60 - 80	23 - 31
G5	GC	19,5	0,30	28 - 32	2 - 10	40 - 60	15 - 23
Soil parameters in Table A.2 correspond to the index of relative density I_D > 0,67							

Table A.3 Fine-grained soils								
Class	Symbol	Soil State	γ [kN/m^3]	ν [-]	φ [°]	c [kPa]	E_{ref} [MPa]	G_{ref} [MPa]
F1	MG	EFF-D [1)]	19,0	0,35	26 - 32	12 - 16	15 - 30	5,6 - 11,1
		EFF-W [2)]	10,9			8 - 16	12 - 21	4,4 - 7,8
		TOT-D [3)]	19,0		12 - 15	70 - 80	30 - 60	11,1 - 22,2
		TOT-W [4)]			10	70	24 - 42	8,9 - 15,6
F2	CG	EFF-D	19,5	0,35	24 - 30	18 - 36	18 - 25	6,7 - 9,3
		EFF-W	11,5			10 - 18	10 - 12	3,7 - 4,4
		TOT-D	19,5		12 - 15	60 - 70	36 - 50	13,3 - 18,5
		TOT-W			10	60	20 - 24	7,4 - 8,9
F3	MS	EFF-D	18,0	0,35	24 - 29	20 - 40	12 - 15	4,4 - 5,6
		EFF-W	9,8			12 - 20	8 - 12	3,0 - 4,4
		TOT-D	18,0		12 - 15	60 - 70	24 - 30	8,9 - 11,1
		TOT-W			10	60	16 - 24	5,9 - 8,9
F4	CS	EFF-D	18,5	0,35	22 - 27	22 - 44	8 - 12	3,0 - 4,4
		EFF-W	10,4			14 - 22	5 - 8	1,9 - 3,0
		TOT-D	18,5		8 - 14	70 - 80	16 - 24	5,9 - 8,9
		TOT-W			5	70	10 - 16	3,7 - 5,9
F5	ML, MI	EFF-D	20,0	0,40	19 - 23	20 - 40	7 - 10	2,5 - 3,5
		EFF-W	12,0			12 - 20	5 - 8	1,8 - 2,9
		TOT-D	20,0		8 - 14	70 - 80	14 - 20	5,0 - 7,0
		TOT-W			5	70	10 - 16	3,6 - 5,6
F6	CL, CI	EFF-D	21,0	0,40	17 - 21	20 - 40	8 - 12	2,9 - 4,3
		EFF-W	13,1			12 - 20	6 - 8	2,1 - 2,9
		TOT-D	21,0		4 - 12	80 - 90	16 - 24	5,7 - 8,6
		TOT-W			0	80	12 - 16	4,3 - 5,7

Soil parameters in Table A.3 correspond to the fine-grained soils with the firm consistency

[1)] Effective parameters for degree of saturation S_r < 0,8

[2] Effective parameters for degree of saturation S_r > 0,8

[3)] Total parameters for degree of saturation S_r < 0,8

[4)] Total parameters for degree of saturation S_r > 0,8

ANNEX B – FACTORS A, B, C, D

Table B.1 Factors A, B, C, D for the sandy soils												
Point	Factor	Height of the abutment H_a [m]										
		2	3	4	5	6	7	8	9	10	12	15
1	A_1	-34,0	-25,0	-16,0	-12,3	-8,5	-6,8	-5,2	-3,9	-2,7	-1,3	-0,3
	B_1	15,5	12,1	8,7	7,1	5,5	4,8	4,1	3,7	3,3	2,7	2,3
	C_1	0,0	0,0	0,0	0,0	0,0	0,0	0,0	0,0	0,0	0,0	0,0
	D_1	0,0	0,0	0,0	0,0	0,0	0,0	0,0	0,0	0,0	0,0	0,0
2R	A_2	-73,0	-53,0	-33,0	-23,8	-14,6	-9,0	-3,4	-1,7	0,0	0,0	0,0
	B_2	42,5	34,7	27,0	23,0	19,0	16,3	13,5	12,0	10,5	9,0	7,8
	C_2	0,0	0,0	0,0	0,0	0,0	0,0	0,0	0,0	0,0	0,0	0,0
	D_2	1,3	1,2	1,1	1,0	0,9	0,8	0,7	0,6	0,5	0,3	0,0
3T	A_3	-67,1	-52,0	-37,0	-29,3	-21,6	-17,9	-14,1	-11,6	-9,1	-5,2	-0,9
	B_3	36,0	30,0	23,9	21,3	18,7	17,2	15,8	14,8	13,9	12,3	10,6
	C_3	1,8	1,7	1,5	1,4	1,2	1,1	1,0	0,8	0,7	0,4	0,0
	D_3	1,0	0,9	0,8	0,8	0,7	0,6	0,5	0,5	0,4	0,2	0,0
z_2	A_z	-0,4	-0,1	0,2	0,5	0,8	1,1	1,4	1,7	2,0	2,6	3,5
	B_z	0,5	0,4	0,4	0,3	0,3	0,3	0,2	0,2	0,1	0,1	-0,1
	C_z	2,7	2,5	2,2	2,0	1,8	1,5	1,3	1,1	0,9	0,4	-0,3
	D_z	0,1	0,2	0,3	0,4	0,5	0,6	0,8	0,9	1,0	1,2	1,5

Table B.2 Factors A, B, C, D for the gravelly soils												
Point	Factor	Height of the abutment H_a [m]										
		2	3	4	5	6	7	8	9	10	12	15
1	A_1	-11,9	-11,1	-10,3	-9,5	-8,7	-7,9	-7,1	-6,2	-5,4	-3,8	-1,4
	B_1	4,3	4,2	4,0	3,9	3,7	3,6	3,4	3,3	3,1	2,8	2,4
	C_1	-14,0	-9,7	-5,5	-3,0	-0,6	0,7	2,0	2,2	2,3	1,4	-0,7
	D_1	5,0	3,9	2,8	2,1	1,4	0,9	0,5	0,4	0,3	0,3	0,5
2R	A_2	-73,2	-61,7	-50,2	-40,8	-31,5	-25,4	-19,2	-15,6	-12,0	-5,9	0,0
	B_2	27,2	24,1	21,0	18,6	16,3	14,9	13,4	12,4	11,4	9,9	8,5
	C_2	-2,2	1,3	4,8	5,8	6,8	6,5	6,2	5,4	4,5	2,8	0,0
	D_2	10,4	7,6	4,8	3,6	2,3	1,7	1,0	0,5	0,0	0,0	0,0
3T	A_3	-55,6	-52,1	-48,7	-45,2	-41,8	-41,8	-41,8	-34,9	-28,1	-21,2	-10,9
	B_3	22,7	21,7	20,7	19,7	18,7	18,7	18,7	16,7	14,7	12,7	9,7
	C_3	-24,1	-12,2	-0,3	4,4	9,1	9,1	9,1	10,9	12,7	9,8	4,5
	D_3	12,1	8,5	4,8	3,2	1,6	1,6	1,6	1,1	0,7	1,1	2,5
z_2	A_z	-0,3	-0,1	0,1	0,3	0,5	0,7	0,9	1,1	1,3	1,7	2,3
	B_z	0,1	0,1	0,1	0,1	0,1	0,1	0,0	0,0	0,0	0,0	0,0
	C_z	2,8	2,7	2,6	2,4	2,3	2,2	2,1	1,9	1,8	1,6	1,2
	D_z	0,5	0,6	0,6	0,7	0,8	0,9	0,9	1,0	1,1	1,2	1,5

ANNEX C – FACTORS K, L, M, N

Table C.1 Factors K, L, M, N for sandy soils										
Soil	Factor	Footing dimensions B_f x L_f [m]								Multiplier
		3x6	4x6	6x6	8x6	3x32	4x32	6x32	8x32	
	K	773	766	752	738	499	498	496	493	10
S1	L	95	103	120	137	65	78	103	128	1
(SW)	M	11,32	8,70	7,51	6,90	9,26	7,11	5,32	4,46	1
	N	75,0	75,0	75,0	75,0	75,0	75,0	75,0	75,0	1
	K	308	307	304	301	225	218	203	189	10
S2	L	57	62	71	80	56	56	57	58	1
(SP)	M	4,68	4,01	3,40	2,94	3,95	3,20	2,49	2,24	1
	N	40,0	40,0	40,0	40,0	40,0	40,0	40,0	40,0	1
	K	128	128	129	130	95	94	93	91	10
S3	L	29	33	40	47	29	32	37	41	1
(SF)	M	2,00	1,91	1,63	1,36	1,95	1,49	1,12	0,98	1
	N	21,0	21,0	21,0	21,0	21,0	21,0	21,0	21,0	1
	K	68	67	65	63	48	46	43	41	10
S4	L	21	25	31	37	15	17	22	26	1
(SM)	M	0,84	0,80	0,74	0,67	0,75	0,69	0,57	0,44	1
	N	10,0	10,0	10,0	10,0	10,0	10,0	10,0	10,0	1
	K	68	67	65	63	48	46	43	41	10
S5	L	21	25	31	37	15	17	22	26	1
(SC)	M	0,84	0,80	0,74	0,67	0,75	0,69	0,57	0,44	1
	N	10,0	10,0	10,0	10,0	10,0	10,0	10,0	10,0	1

Table C.2 Factors K, L, M, N for gravelly soils										
Soil	Factor	Footing dimensions B_f x L_f [m]								Multiplier
		3x6	4x6	6x6	8x6	3x32	4x32	6x32	8x32	
	K	3970	3900	3750	3610	2190	2210	2260	2320	10
G1	L	130	134	142	150	68	81	106	132	1
(GW)	M	51,20	42,18	34,57	31,35	43,76	33,05	22,50	19,62	1
	N	430,0	430,0	430,0	430,0	430,0	430,0	430,0	430,0	1
	K	1600	1600	1600	1610	920	920	930	940	10
G2	L	100	109	127	144	58	67	84	101	1
(GP)	M	21,15	17,63	14,32	12,44	18,73	15,73	10,89	8,64	1
	N	210,0	210,0	210,0	210,0	210,0	210,0	210,0	210,0	1
	K	780	780	780	780	480	480	480	480	10
G3	L	70	79	97	115	48	54	67	80	1
(GF)	M	9,06	7,86	6,87	6,53	7,50	6,80	4,78	4,00	1
	N	95,0	95,0	95,0	95,0	95,0	95,0	95,0	95,0	1
	K	633	631	627	624	403	395	379	363	10
G4	L	52	59	74	88	36	40	50	60	1
(GM)	M	6,72	6,18	5,08	3,99	6,42	5,77	4,48	3,18	1
	N	70,0	70,0	70,0	70,0	70,0	70,0	70,0	70,0	1
	K	391	409	444	479	251	256	266	276	10
G5	L	28	38	59	80	14	23	40	58	1
(GC)	M	4,73	4,03	2,62	1,22	4,51	3,92	2,74	1,56	1
	N	50,0	50,0	50,0	50,0	50,0	50,0	50,0	50,0	1

Table C.3 Factors K, L, M, N for fine-grained soils with effective parameters										
Soil	Factor	Footing dimensions B_f x L_f [m]								Multiplier
		3x6	4x6	6x6	8x6	3x32	4x32	6x32	8x32	
F1 (MG)	K	136	128	112	96	111	101	82	63	10
	L	62	57	46	36	54	48	36	25	1
	M	6,88	5,49	4,44	4,19	4,72	3,86	3,15	2,58	1
	N	21,5	21,5	21,5	21,5	21,5	21,5	21,5	21,5	1
F2 (CG)	K	136	128	112	96	111	101	82	63	10
	L	62	57	46	36	54	48	36	25	1
	M	6,88	5,49	4,44	4,19	4,72	3,86	3,15	2,58	1
	N	21,5	21,5	21,5	21,5	21,5	21,5	21,5	21,5	1
F3 (MS)	K	79	74	64	55	60	56	47	37	10
	L	62	57	46	36	54	48	36	25	1
	M	4,46	3,59	2,80	2,70	3,25	2,62	1,96	1,72	1
	N	13,5	13,5	13,5	13,5	13,5	13,5	13,5	13,5	1
F4 (CS)	K	67	62	52	43	51	45	35	24	10
	L	62	57	46	36	54	48	36	25	1
	M	2,90	2,20	1,76	1,80	2,13	1,70	1,40	1,29	1
	N	10,0	10,0	10,0	10,0	10,0	10,0	10,0	10,0	1
F5 (ML, MI)	K	67	62	52	43	51	45	35	24	10
	L	62	57	46	36	54	48	36	25	1
	M	2,90	2,20	1,76	1,80	2,13	1,70	1,40	1,29	1
	N	9,5	9,5	9,5	9,5	9,5	9,5	9,5	9,5	1
F6 (CL, CI)	K	67	62	52	43	51	45	35	24	10
	L	62	57	46	36	54	48	36	25	1
	M	2,90	2,20	1,76	1,80	2,13	1,70	1,40	1,29	1
	N	10,3	10,3	10,3	10,3	10,3	10,3	10,3	10,3	1

Table C.4 Factors K, L, M, N for fine-grained soils with total parameters										
Soil	Factor	Footing dimensions B_f x L_f [m]								Multiplier
		3x6	4x6	6x6	8x6	3x32	4x32	6x32	8x32	
F1 (MG)	K	233	217	184	151	173	161	138	114	10
	L	46	41	31	21	41	37	28	20	1
	M	15,71	12,30	10,31	9,59	11,42	8,95	6,72	5,78	1
	N	43,0	43,0	43,0	43,0	43,0	43,0	43,0	43,0	1
F2 (CG)	K	233	217	184	151	173	161	138	114	10
	L	46	41	31	21	41	37	28	20	1
	M	15,71	12,30	10,31	9,59	11,42	8,95	6,72	5,78	1
	N	43,0	43,0	43,0	43,0	43,0	43,0	43,0	43,0	1
F3 (MS)	K	146	135	114	92	118	108	89	70	10
	L	46	41	31	21	41	37	28	20	1
	M	9,76	7,56	6,23	5,95	6,77	5,50	4,11	3,59	1
	N	27,0	27,0	27,0	27,0	27,0	27,0	27,0	27,0	1
F4 (CS)	K	99	91	76	60	78	72	60	48	10
	L	46	41	31	21	41	37	28	20	1
	M	7,41	5,83	4,71	4,47	5,40	4,38	3,18	2,69	1
	N	20,0	20,0	20,0	20,0	20,0	20,0	20,0	20,0	1
F5 (ML, MI)	K	99	91	76	60	78	72	60	48	10
	L	46	41	31	21	41	37	28	20	1
	M	7,41	5,83	4,71	4,47	5,40	4,38	3,18	2,69	1
	N	19,0	19,0	19,0	19,0	19,0	19,0	19,0	19,0	1
F6 (CL, CI)	K	99	91	76	60	78	72	60	48	10
	L	46	41	31	21	41	37	28	20	1
	M	7,41	5,83	4,71	4,47	5,40	4,38	3,18	2,69	1
	N	20,5	20,5	20,5	20,5	20,5	20,5	20,5	20,5	1

ANNEX D – FACTORS P, Q, R, S, T, U

Table D.1 Factors P, Q, R, S, T, U for sandy soils										
Soil	Factor	Footing dimensions B_f x L_f [m]								Multiplier
		3x6	4x6	6x6	8x6	3x32	4x32	6x32	8x32	
S1 (SW)	P	9,77	6,74	5,35	4,64	6,53	4,45	3,17	2,25	0,001
	Q	13,40	9,01	6,35	5,28	9,53	6,31	3,92	3,06	1
	R	100,0	100,0	100,0	100,0	100,0	100,0	100,0	100,0	1
	S	12,6	9,5	8,1	7,5	9,0	7,1	5,7	5,0	0,001
	T	29,3	23,5	19,8	18,0	22,2	18,4	14,5	12,3	1
	U	29,3	29,3	29,3	29,3	29,3	29,3	29,3	29,3	1
S2 (SP)	P	9,77	6,74	5,35	4,64	6,53	4,45	3,17	2,25	0,001
	Q	8,10	5,88	4,63	3,63	5,87	4,35	2,95	2,05	1
	R	75,0	75,0	75,0	75,0	75,0	75,0	75,0	75,0	1
	S	12,6	9,5	8,1	7,5	9,0	7,1	5,7	5,0	0,001
	T	16,4	13,2	11,3	10,3	12,6	10,3	8,2	7,1	1
	U	15,6	15,6	15,6	15,6	15,6	15,6	15,6	15,6	1
S3 (SF)	P	9,77	6,74	5,35	4,64	6,53	4,45	3,17	2,25	0,001
	Q	4,85	3,65	2,55	2,05	3,50	2,63	1,85	1,23	1
	R	50,0	50,0	50,0	50,0	50,0	50,0	50,0	50,0	1
	S	12,6	9,5	8,1	7,5	9,0	7,1	5,7	5,0	0,001
	T	9,4	7,7	6,5	5,9	7,3	6,0	4,8	4,1	1
	U	8,1	8,1	8,1	8,1	8,1	8,1	8,1	8,1	1
S4 (SM)	P	9,77	6,74	5,35	4,64	6,53	4,45	3,17	2,25	0,001
	Q	1,50	0,98	0,90	0,71	1,16	0,95	0,65	0,41	1
	R	37,5	37,5	37,5	37,5	37,5	37,5	37,5	37,5	1
	S	12,6	9,5	8,1	7,5	9,0	7,1	5,7	5,0	0,001
	T	5,0	4,1	3,5	3,3	3,9	3,3	2,6	2,3	1
	U	3,8	3,8	3,8	3,8	3,8	3,8	3,8	3,8	1
S5 (SC)	P	9,77	6,74	5,35	4,64	6,53	4,45	3,17	2,25	0,001
	Q	1,50	0,98	0,90	0,71	1,16	0,95	0,65	0,41	1
	R	25,0	25,0	25,0	25,0	25,0	25,0	25,0	25,0	1
	S	12,6	9,5	8,1	7,5	9,0	7,1	5,7	5,0	0,001
	T	5,0	4,1	3,5	3,3	3,9	3,3	2,6	2,3	1
	U	3,8	3,8	3,8	3,8	3,8	3,8	3,8	3,8	1

Table D.2 Factors P, Q, R, S, T, U for gravelly soils										
Soil	Factor	Footing dimensions B_f x L_f [m]								Multiplier
		3x6	4x6	6x6	8x6	3x32	4x32	6x32	8x32	
G1 (GW)	P	37,2	34,5	29,2	23,8	24,3	22,5	18,9	15,4	0,001
	Q	73,4	56,0	44,2	34,9	47,8	40,6	30,5	23,5	1
	R	150,0	150,0	150,0	150,0	150,0	150,0	150,0	150,0	1
	S	40,1	38,4	35,0	31,6	24,7	24,1	22,8	21,5	0,001
	T	152,7	121,7	105,7	96,4	106,9	89,8	74,6	64,7	1
	U	179,2	179,2	179,2	179,2	179,2	179,2	179,2	179,2	1
G2 (GP)	P	27,5	24,7	19,3	13,9	15,7	14,6	12,4	10,2	0,001
	Q	41,1	30,0	23,1	19,2	25,4	21,1	16,9	13,2	1
	R	125,0	125,0	125,0	125,0	125,0	125,0	125,0	125,0	1
	S	31,6	29,0	23,9	18,7	18,4	17,4	15,5	13,5	0,001
	T	76,9	61,1	52,3	48,2	53,7	45,4	37,9	32,7	1
	U	87,5	87,5	87,5	87,5	87,5	87,5	87,5	87,5	1
G3 (GF)	P	16,6	14,9	11,7	8,5	10,4	9,4	7,3	5,1	0,001
	Q	19,6	14,8	11,4	9,5	13,1	10,9	7,9	6,1	1
	R	100,0	100,0	100,0	100,0	100,0	100,0	100,0	100,0	1
	S	20,2	18,6	15,4	12,2	13,8	12,7	10,6	8,5	0,001
	T	36,0	29,0	24,7	22,7	26,7	22,6	17,9	15,3	1
	U	38,0	38,0	38,0	38,0	38,0	38,0	38,0	38,0	1
G4 (GM)	P	11,3	10,4	8,6	6,8	6,8	6,1	4,8	3,4	0,001
	Q	13,2	10,1	7,7	5,9	9,3	7,4	5,0	3,4	1
	R	75,0	75,0	75,0	75,0	75,0	75,0	75,0	75,0	1
	S	20,2	18,6	15,4	12,2	13,8	12,7	10,6	8,5	0,001
	T	29,6	24,0	20,3	18,3	22,6	18,7	14,9	12,4	1
	U	26,9	26,9	26,9	26,9	26,9	26,9	26,9	26,9	1
G5 (GC)	P	8,4	7,4	5,4	3,4	3,2	3,2	3,1	3,1	0,001
	Q	7,5	5,7	3,8	3,0	5,4	4,3	2,5	2,2	1
	R	50,0	50,0	50,0	50,0	50,0	50,0	50,0	50,0	1
	S	20,2	18,6	15,4	12,2	13,8	12,7	10,6	8,5	0,001
	T	23,6	19,4	16,0	14,7	17,6	15,2	11,8	10,2	1
	U	19,2	19,2	19,2	19,2	19,2	19,2	19,2	19,2	1

Table D.3 Factors P, Q, R, S, T, U for fine-grained soils with effective parameters										
Soil	Factor	Footing dimensions B_f x L_f [m]								Multiplier
		3x6	4x6	6x6	8x6	3x32	4x32	6x32	8x32	
F1 (MG)	P	0,0	0,0	0,0	0,0	0,0	0,0	0,0	0,0	-
	Q	0,89	0,73	0,40	0,07	0,77	0,63	0,34	0,05	1
	R	50,0	50,0	50,0	50,0	50,0	50,0	50,0	50,0	1
	S	6,6	6,1	5,2	4,2	5,1	4,7	3,9	3,0	0,001
	T	9,6	7,8	6,3	5,7	7,5	6,2	4,6	4,0	1
	U	8,5	8,5	8,5	8,5	8,5	8,5	8,5	8,5	1
F2 (CG)	P	0,0	0,0	0,0	0,0	0,0	0,0	0,0	0,0	-
	Q	0,89	0,73	0,40	0,07	0,77	0,63	0,34	0,05	1
	R	38,0	38,0	38,0	38,0	38,0	38,0	38,0	38,0	1
	S	6,6	6,1	5,2	4,2	5,1	4,7	3,9	3,0	0,001
	T	9,6	7,8	6,3	5,7	7,5	6,2	4,6	4,0	1
	U	8,5	8,5	8,5	8,5	8,5	8,5	8,5	8,5	1
F3 (MS)	S	6,6	6,1	5,2	4,2	5,1	4,7	3,9	3,0	0,001
	T	5,9	4,9	4,0	3,6	4,7	3,8	3,0	2,6	1
	U	5,0	5,0	5,0	5,0	5,0	5,0	5,0	5,0	1
F4 (CS)	S	6,6	6,1	5,2	4,2	5,1	4,7	3,9	3,0	0,001
	T	4,4	3,6	3,0	2,7	3,6	2,8	2,2	1,9	1
	U	3,5	3,5	3,5	3,5	3,5	3,5	3,5	3,5	1
F5 (ML, MI)	S	6,6	6,1	5,2	4,2	5,1	4,7	3,9	3,0	0,001
	T	3,8	3,1	2,6	2,4	3,0	2,4	1,9	1,5	1
	U	3,0	3,0	3,0	3,0	3,0	3,0	3,0	3,0	1
F6 (CL, CI)	S	6,6	6,1	5,2	4,2	5,1	4,7	3,9	3,0	0,001
	T	3,8	3,1	2,6	2,4	3,0	2,4	1,9	1,5	1
	U	3,0	3,0	3,0	3,0	3,0	3,0	3,0	3,0	1

Table D.4 Factors P, Q, R, S, T, U for fine-grained soils with total parameters										
Soil	Factor	Footing dimensions B_f x L_f [m]								Multiplier
		3x6	4x6	6x6	8x6	3x32	4x32	6x32	8x32	
F1 (MG)	P	0,0	0,0	0,0	0,0	0,0	0,0	0,0	0,0	-
	Q	1,10	0,93	0,58	0,24	1,05	0,86	0,46	0,07	1
	R	50,0	50,0	50,0	50,0	50,0	50,0	50,0	50,0	1
	S	13,2	12,3	10,5	8,6	9,7	9,0	7,7	6,4	0,001
	T	19,5	15,5	12,6	11,5	15,0	12,3	9,5	7,9	1
	U	17,0	17,0	17,0	17,0	17,0	17,0	17,0	17,0	1
F2 (CG)	P	0,0	0,0	0,0	0,0	0,0	0,0	0,0	0,0	-
	Q	1,10	0,93	0,58	0,24	1,05	0,86	0,46	0,07	1
	R	38,0	38,0	38,0	38,0	38,0	38,0	38,0	38,0	1
	S	13,2	12,3	10,5	8,6	9,7	9,0	7,7	6,4	0,001
	T	19,5	15,5	12,6	11,5	15,0	12,3	9,5	7,9	1
	U	17,0	17,0	17,0	17,0	17,0	17,0	17,0	17,0	1
F3 (MS)	S	13,2	12,3	10,5	8,6	9,7	9,0	7,7	6,4	0,001
	T	12,1	9,6	7,8	7,1	9,2	7,5	5,8	4,9	1
	U	10,0	10,0	10,0	10,0	10,0	10,0	10,0	10,0	1
F4 (CS)	S	13,2	12,3	10,5	8,6	9,7	9,0	7,7	6,4	0,001
	T	9,0	7,3	5,9	5,3	7,0	5,8	4,3	3,7	1
	U	7,0	7,0	7,0	7,0	7,0	7,0	7,0	7,0	1
F5 (ML, MI)	S	13,2	12,3	10,5	8,6	9,7	9,0	7,7	6,4	0,001
	T	7,5	6,1	5,2	4,7	5,9	4,8	3,8	3,4	1
	U	6,0	6,0	6,0	6,0	6,0	6,0	6,0	6,0	1
F6 (CL, CI)	S	13,2	12,3	10,5	8,6	9,7	9,0	7,7	6,4	0,001
	T	7,5	6,1	5,2	4,7	5,9	4,8	3,8	3,4	1
	U	6,0	6,0	6,0	6,0	6,0	6,0	6,0	6,0	1

ANNEX E – FACTORS W_Z AND W_X

Table E.1 Factors W_z and W_x				
Soil	W_z		W_x	
	Above GWL	Below GWL	Above GWL	Below GWL
S1 (SW)	1,00	0,65	1,00	0,75
S2 (SP)	1,00	0,65	1,00	0,75
S3 (SF)	1,00	0,70	1,00	0,80
S4 (SM)	1,00	0,75	1,00	0,85
S5 (SC)	1,00	0,75	1,00	0,85
G1 (GW)	1,00	0,70	1,00	0,75
G2 (GP)	1,00	0,70	1,00	0,80
G3 (GF)	1,00	0,75	1,00	0,80
G4 (GM)	1,00	0,75	1,00	0,80
G5 (GC)	1,00	0,75	1,00	0,85
F1 (MG) [1)]	1,00	0,55	1,00	0,65
F2 (CG) [1)]	1,00	0,40	1,00	0,45
F3 (MS) [1)]	1,00	0,60	1,00	0,65
F4 (CS) [1)]	1,00	0,50	1,00	0,55
F5 (ML, MI) [1)]	1,00	0,60	1,00	0,65
F6 (CL, CI) [1)]	1,00	0,55	1,00	0,60
F1 (MG) [2)]	1,00	0,70	1,00	0,75
F2 (CG) [2)]	1,00	0,50	1,00	0,50
F3 (MS) [2)]	1,00	0,75	1,00	0,75
F4 (CS) [2)]	1,00	0,65	1,00	0,65
F5 (ML, MI) [2)]	1,00	0,75	1,00	0,75
F6 (CL, CI) [2)]	1,00	0,70	1,00	0,70
[1)] Soil with effective parameters, [2)] Soil with total parameters				

ANNEX F – DEPTH OF COMPRESSIBLE SUBSOIL H_S

Table F.1 Depth of compressible subsoil H_s [m]									
Soil	f_z	Footing dimensions B_f x L_f [m]							
	[kPa]	3x6	4x6	6x6	8x6	3x32	4x32	6x32	8x32
S1 (SW)	200	4,9	5,5	6,4	7,1	6,4	7,2	8,5	9,4
	400	6,5	7,4	8,5	9,4	8,5	9,5	11,3	12,6
	800	8,6	9,8	11,3	12,5	11,3	12,7	15,1	16,8
S2 (SP)	150	4,9	5,5	6,4	7,1	5,6	6,3	7,5	8,3
	300	6,1	7,0	8,1	8,9	7,6	8,6	10,2	11,3
	600	7,7	8,8	10,2	11,3	10,4	11,6	13,9	15,4
S3 (SF)	100	4,1	4,7	5,4	6,0	4,9	5,5	6,5	7,2
	200	5,7	6,4	7,4	8,2	6,5	7,3	8,7	9,7
	400	7,8	8,8	10,2	11,3	8,8	9,8	11,7	13,0
S4 (SM)	75	3,4	3,8	4,4	4,9	3,9	4,3	5,2	5,7
	150	4,7	5,4	6,2	6,9	5,5	6,1	7,3	8,1
	300	6,7	7,6	8,7	9,7	7,7	8,6	10,3	11,4
S5 (SC)	50	2,6	3,0	3,4	3,8	3,4	3,8	4,5	5,0
	100	3,7	4,2	4,9	5,4	4,8	5,4	6,4	7,1
	200	5,3	6,0	6,9	7,7	6,9	7,7	9,2	10,2
G1 (GW)	300	5,6	6,7	7,6	8,3	7,1	8,2	9,4	10,7
	600	7,2	8,5	9,7	10,6	9,5	11,0	12,6	14,3
	1200	9,1	10,8	12,3	13,6	12,8	14,7	16,8	19,2
G2 (GP)	250	5,6	6,7	7,6	8,3	7,1	8,2	9,4	10,7
	500	7,0	8,3	9,5	10,4	9,6	11,0	12,6	14,4
	1000	8,8	10,4	11,8	13,1	12,8	14,7	16,9	19,2
G3 (GF)	200	4,9	5,8	6,6	7,2	6,4	7,3	8,4	9,6
	400	6,5	7,6	8,7	9,6	8,7	10,1	11,5	13,1
	800	8,5	10,1	11,5	12,7	12,0	13,8	15,8	18,0
G4 (GM)	150	4,9	5,8	6,6	7,2	5,6	6,5	7,4	8,5
	300	6,5	7,7	8,7	9,6	7,4	8,5	9,8	11,2
	600	8,7	10,3	11,7	12,8	9,8	11,3	12,9	14,7
G5 (GC)	100	4,1	4,9	5,6	6,1	4,9	5,6	6,4	7,3
	200	5,5	6,6	7,5	8,2	6,5	7,5	8,6	9,7
	400	7,4	8,8	10,0	11,0	8,6	9,9	11,4	13,0
F1 (MG)	100	4,9	5,7	6,3	7,1	5,6	6,5	7,5	8,4
	200	6,5	7,7	8,4	9,4	7,5	8,6	10,0	11,1
	400	8,7	10,2	11,2	12,5	9,9	11,4	13,2	14,8
F2 (CG)	75	4,1	4,9	5,3	6,0	4,9	5,6	6,5	7,3
	150	5,7	6,7	7,4	8,2	6,6	7,6	8,8	9,9
	300	7,9	9,3	10,2	11,4	9,0	10,3	12,0	13,4
F3 (MS)	75	4,1	4,9	5,3	6,0	4,9	5,6	6,5	7,3
	150	5,6	6,6	7,3	8,2	6,8	7,7	9,0	10,1
	300	7,7	9,1	10,0	11,2	9,4	10,7	12,5	13,9
F4 (CS)	75	4,1	4,9	5,3	6,0	4,9	5,6	6,5	7,3
	150	5,7	6,7	7,4	8,3	6,7	7,7	8,9	10,0
	300	7,9	9,3	10,2	11,4	9,2	10,6	12,3	13,7
F5 (ML, MI)	75	4,1	4,9	5,3	6,0	4,9	5,6	6,5	7,3
	150	5,7	6,7	7,3	8,2	6,6	7,5	8,8	9,8
	300	7,7	9,1	10,0	11,2	8,9	10,2	11,8	13,2
F6 (CL, CI)	50	3,4	4,0	4,4	4,9	4,1	4,7	5,5	6,1
	100	4,7	5,5	6,1	6,8	5,8	6,6	7,7	8,6
	200	6,5	7,7	8,4	9,4	8,1	9,3	10,8	12,0

ANNEX G – LIMIT STRESS IN FOOTING BOTTOM

Table G.1 Limit vertical and horizontal stress in the footing bottom $f_{z, lim}$ and $f_{x, lim}$		
Soil	$f_{z, lim}$ [kPa]	$f_{x, lim}$ [kPa]
S1 (SW)	800	100,0
S2 (SP)	600	75,0
S3 (SF)	400	50,0
S4 (SM)	300	37,5
S5 (SC)	200	25,0
G1 (GW)	1200	150,0
G2 (GP)	1000	125,0
G3 (GF)	800	100,0
G4 (GM)	600	75,0
G5 (GC)	400	50,0
F1 (MG)	400	50,0
F2 (CG)	300	37,5
F3 (MS)	300	37,5
F4 (CS)	300	37,5
F5 (ML, MI)	300	37,5
F6 (CL, CI)	200	25,0

LITERATURE

Standards and Regulations

[1] **BA 42/96 Part 12:** The Design of Integral Bridges, Highways Agency, 2003.

[2] **ČSN 73 1001:** Foundation of Structures. Subsoil under shallow Foundations, Český normalizační institut, 1987.

[3] **EN 1990:** Basis of Structural Design, CEN, 2004.

[4] **EN 1991-1-5:** Actions on Structures. General Actions – Thermal Actions, CEN, 2005.

[5] **EN 1991-2:** Actions on Structures. Traffic Loads on Bridges, CEN, 2005.

Publications

[6] **Biddle, A. R. – Iles, D. C. – Yandzio, E.:** Integral Steel Bridges – Design Guidance, The Steel Construction Institute, 1997.

[7] **Braun, A. – Seidl, G. – Weizenegger, M.:** Rahmentragwerke im Brückenbau – Konstruktion, Berechnung und Volkwitschaftliche Betrachtung, Beton- und Stahlbetonbau, 2006, roč. 101, č. 3, str. 187 – 197.

[8] **Buba, R. – Stumpf, D.:** Integrální železniční mosty v SRN a jejich výhody pro minimalizaci doby výluk, Sborník konference Železniční mosty a tunely, 2007, str. 25-30.

[9] **Collin, P. – Lundmark, T.:** Competitive Swedish Composite Bridges, IABSE Melbourne, 2002.

[10] **Collin, P. – Stoltz, A. – Moller, M.:** Innovative Prefabricated Composite Bridges, IABSE Melbourne, 2002.

[11] **Engelsmann, S. – Schlaich, J. – Schäfer, K:** Deutscher Ausschluss für Stahlbeton – Entwerfen und Bemessen von Betonbrücken ohne Fugen und Lager, Beuth Verlag, 1999.

[12] **Iles, D. C. – Yandzio, E.:** Integral Bridges in the UK, The Steel Construction Institute, 2006.

[13] **Jung, J. H. – Jang, W. S. – You, S. K. – Kim, Y. H. – Yoon, S. J.:** Development of Preflex Composite Beam-Stub Abutment Integral Bridge System, International Journal of Steel Structures, 2006, roč. 6, č. 3, str. 175 – 181.

[14] **Krizek, J.:** Integral Bridges, Doctoral thesis, Prague, 2009.

[15] **Lamboj, L. – Studnička, J.:** Integrované ocelobetonové silniční mosty. Stavební obzor, 1999, č 2.

[16] **Nicholson, B. A.:** Integral Abutments for Prestressed Beam Bridges, Prestressed Concrete Association, 1998.

[17] **Petursson, H. – Collin, P.:** Composite Bridges with Integral Abutments Minimizing Lifetime Costs, Sborník symposia IABSE, Melbourne, 2002.

[18] **Schmitt, V. – Buba, R.:** Innovative Building Methods for Bridges with Small and Medium Spans – VFT and VFT-WIB, Sborník konference Steel Bridges, Praha, 2006, str. 66 – 74.

[19] **Schüller, M.:** Konzeptionelles Entwerfen und Konstruieren von Integralen Betonbrücken – Entwicklung, Bedeutung und Beispiele, Beton- und Stahlbetonbau, 2004, roč. 99, č. 10, str. 774 – 789.

[20] **Strauß, P – Hensel, B.:** Schiefes, Vorgespanntes Rahmentragwerk an der Anschlussstelle Erfurt-West der BAB 4, Sborník 11. Dresdner Brückenbausymposium, Dresden, 2001, str. 61 – 77.

[21] **Weizenegger, M.:** Hybrid Frame Bridge, River Saale, Merseburg, Germany, Structural Engineering International, IABSE, 2003, roč. 13, č. 3, str. 179 – 181.

[22] **Zordan, T. – Briseghella, B.:** Attainment of an integral Abutment Bridge through the Refubrishment of a Simply Supported Structure, Structural Engineering International, IABSE, 2007, roč. 17, č. 3, str. 228-234.